JOC The Journal of Organic Chemistry

Article

pubs.acs.org/joc

Diindole-Annulated Naphthalene Diimides: Synthesis and Optical and Electronic Properties of *Syn*- and *Anti*-Isomers

Sabin-Lucian Suraru, Christian Burschka, and Frank Würthner*

Universität Würzburg, Institut für Organische Chemie & Center for Nanosystems Chemistry, Am Hubland, 97074 Würzburg, Germany

Supporting Information

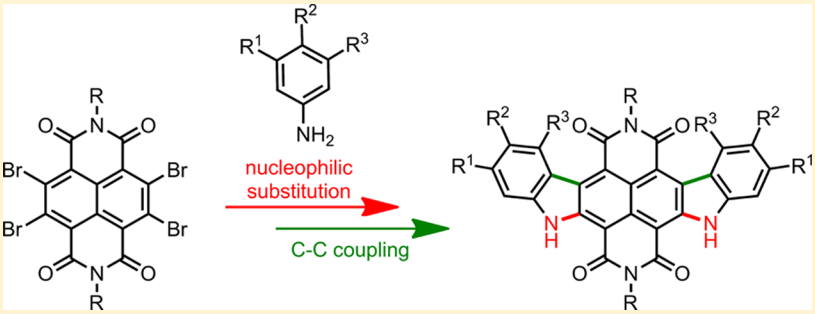

ABSTRACT: Here we report a selective method for the core-extension of naphthalene diimide (NDI) with two annulated indole rings leading to carbazolo[2,3-*b*]carbazole diimides (CbDIs) with exclusive *syn*-connectivity based on a regioselective nucleophilic substitution reaction of Br_4-NDI with arylamines, followed by palladium-catalyzed intramolecular C−C coupling. The oxygen analogues of *anti*-CbDIs, namely *anti*-benzofurobenzofuran diimides (*anti*-BfDIs), were obtained from 2,6-Br_2-NDI and 2-bromophenol. The *syn*- and *anti*-isomers of CbDIs were unambiguously characterized by single-crystal X-ray analysis. The optical properties of the present core-enlarged NDIs were studied, revealing clear differences in the absorption characteristics of the *syn*- and *anti*-isomers of CbDI, on one hand, and CbDI vs BfDI derivatives, on the other hand. Cyclic voltammetry studies showed that the redox properties are dependent on the substituents at the CbDI-core and oxygen atom containing BfDIs are more prone to reduction than the respective nitrogen analogues CbDIs. Vacuum-processed organic field effect transistors reveal CbDI and BfDI derivatives with n-channel, p-channel, as well as ambient transport characteristics with mobility values up to 0.2 $cm^2/(V\ s)$.

INTRODUCTION

The extension of conjugated π-systems is a widely applied approach in the fields of small molecule based organic electronics and photovoltaics.[1−5] This strategy leads to molecules with desirable electronic characteristics such as reduced band gap. Moreover, extension of aromatic systems is often accompanied by an enhanced intermolecular overlap of the π-systems in the bulk, improving electronic coupling between the molecules and thus the charge transport.[6] For these reasons polycyclic aromatic compounds such as acenes[7] have been emerged in the early stage of development as one of the most important class of p-type organic semiconductor materials. However, extension of the conjugated π-systems to linearly fused acenes goes along with a lack of stability and solubility of these compounds and thus several strategies have been applied to circumvent such drawbacks by structural modification. For example, the incorporation of heteroatoms in to the polycyclic conjugated core leading to heteroacenes,[8−14] and functionalization of peri-substituted acenes with bulky silylethinyl groups[15−17] were shown to be very promising in this regard. During the last years, lower homologue rylene diimides, in particular perylene diimides (PDIs) and naphthalene diimides (NDIs), have been developed as highly powerful, air-stable n-type semiconductors due to their good packing behavior and electron-poor character.[18−20]

Motivated by the aforementioned advancements during the past few years, several synthetic strategies have been developed to enlarge the π-core of NDIs, the latter being the smallest acene diimides, leading to core-expanded acene[21−23] and heteroacene-like[24−28] derivatives functionalized with diimide moieties along the short axis of the molecules. Along this line, sulfur-containing core-enlarged NDIs were introduced by Zhu et al. as an outstanding class of solution-processable n-type semiconductors.[29−31] As one of the earlier examples of core-extended NDIs, we reported in our previous communication a carbazolo[2,3-*b*]carbazole-6,7:13,14-tetracarboxylic acid diimide (CbDI) that exhibits ambipolar charge transport behavior with good hole mobility (structure **Ia** in Chart 1).[32] The core enlargement of NDI was achieved by a one-pot, two-step reaction of 2,6-dibromo-NDI (2,6-Br_2-NDI) with 2-bromoaniline. Recently, Wang et al. have reported a sulfur analogue of **Ia**

Received: October 24, 2013
Published: November 26, 2013

   dx.doi.org/10.1021/jo402365s | *J. Org. Chem.* 2014, 79, 128−139

Chart 1

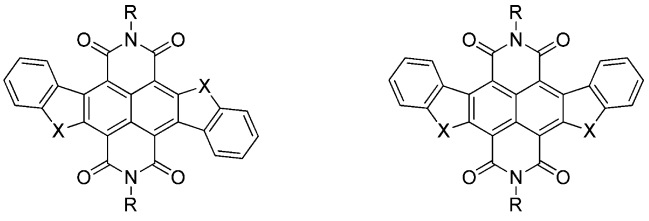

(**Ib** in Chart 1), which was synthesized from the 2,6-distannyl-NDI in three steps.[33] Very recently, Takimiya et al. have achieved the synthetic access to naphthodithiophene diimides, a four-ring annulated analogue to **Ib**, by cyclization of a 2,6-diethynyl-NDI in the presence of sodium sulfide.[34] The aforementioned examples represent core-enlarged NDIs with an inversion symmetry and *anti*-connectivity of the heteroatoms to the NDI core. This constitution derives from the readily accessible 2,6-regioisomer of 2,6-dibromonaphthalene dianhydride (2,6-Br_2-NDA) precursor.[35] However, a selective synthesis of *syn*-isomeric heteroatom-containing ring-annulated NDIs of general structure **II** (shown in Chart 1) has not been reported so far. The reason might be that an analogous route to *syn*-isomers is apparently not very attractive because the required symmetrically positioned 2,7-dihalogenated NDI precursors are not easily accessible.[36]

Herein we present a novel synthetic method for hitherto unknown core-diindole-annulated NDIs with *syn*-connectivity (*syn*-CbDIs) based on highly regioselective nucleophilic substitution of Br_4-NDI at 2,7-positions with aniline,[37] followed by palladium-catalyzed intramolecular C−C coupling (Scheme 1). Furthermore, we have synthesized *anti*-CbDIs (**Ia**, Chart 1) as well as oxygen analogues (**Ic**, Chart 1) and studied the optical and electronic properties of *anti*- and *syn*-isomers in a comparative manner.

RESULTS AND DISCUSSION

Synthesis. Our synthetic route to *syn*-CbDIs is based on our recent observation that nucleophilic substitution of Br_4-NDIs with aniline leads with high regioselectivity to 2,7-diphenylamino-3,6-dibromo-NDIs.[37] Such NDI derivatives possessing carbon−bromine bonds in the NDI core and carbon−hydrogen bonds located at the core-bound phenylamino group in the *ortho*-position to the nitrogen atom should be prone to intramolecular arylation by C−C coupling. Thus, we have synthesized a series of 2,7-diphenylamino-3,6-dibromo-NDIs **1a−f** bearing different substituents in the imide positions and on the phenylamino group by the regioselective nucleophilic substitution reaction of Br_4-NDIs (R = DIPP, C_8H_{17}, C_3H_7) with the respective aniline derivatives in chloroform or toluene. Indeed, the subsequent palladium-catalyzed intramolecular C−C coupling of **1a−f** afforded the respective *syn*-CbDIs **2a−f** (Scheme 1). The reaction of Br_4-NDI-C_8H_{17} in chloroform with excess aniline (ca. 90 equiv) afforded **1b** selectively as the only disubstitution product within 2 h in a yield of 87%. NDI derivative **1a** with a 2,6-diisopropylphenyl (DIPP) group in the imide positions was obtained by the same procedure in 82% yield. With 3- or 4-*tert*-butylaniline the corresponding derivatives **1c** and **1d** were obtained highly regioselectively (2,7-isomer) in 76% yield, respectively. Substitution of Br_4-NDI-C_3H_7 with 3-*tert*-butylaniline gave NDI **1e**, bearing the same substitution pattern at the NDI core as in NDI **1c**. For the reaction of Br_4-NDI-C_8H_{17} with electron-poor and less nucleophilic 3,5-bis(trifluoromethyl)aniline prolonged reaction time was required, and the respective 2,7-diamino-NDI **1f** was obtained after several days of reaction in toluene at 70 °C in 81% yield. Subsequently, the intramolecular cyclization of diaminodibromo-NDIs **1a−f** to the respective *syn*-CbDIs was performed with $Pd(OAc)_2$ as a catalyst and K_2CO_3 as base in DMF. A temperature of 100 °C turned out to be sufficient for these reactions, and derivatives **2a−e** were obtained after 1−1.5 h reaction time in 28−54% yield. However, for the synthesis of CbDI **2f** bearing CF_3 groups a higher temperature (ca. 150 °C) is required.

For the purpose of comparative studies of molecular properties of *syn*- and *anti*-isomers, we have also synthesized the *anti*-CbDIs **3a,b**. The one-pot reaction of 2,6-Br_2-NDI bearing 2,6-diisopropylphenyl substituents in the imide positions with 2-bromoaniline in the presence of $Pd(OAc)_2$ and K_2CO_3 in DMF afforded **3a** in 13% yield (Scheme 2).[32] The *anti*-CbDI derivative **3b** with a branched alkyl chain in the imide positions was synthesized in 10% isolated yield. It is remarkable that in contrast to CbDI **3a**, derivative **3b** lacks of good solubility despite bearing branched 2-ethylhexyl groups. To assess the scope of this synthetic method for NDI-core expansion, we have performed analogous annulation reactions of 2,6-Br_2-NDIs with 2-bromophenol as oxygen nucleophile and obtained the benzofurobenzofuran diimides (BfDIs) **4a** and **4b** with *anti*-connectivity in 16−35% isolated yields (Scheme 2). Remarkably, in contrast to *anti*-CbDI **3a**, *anti*-

Scheme 1. Synthesis of *syn*-CbDIs 2a−f

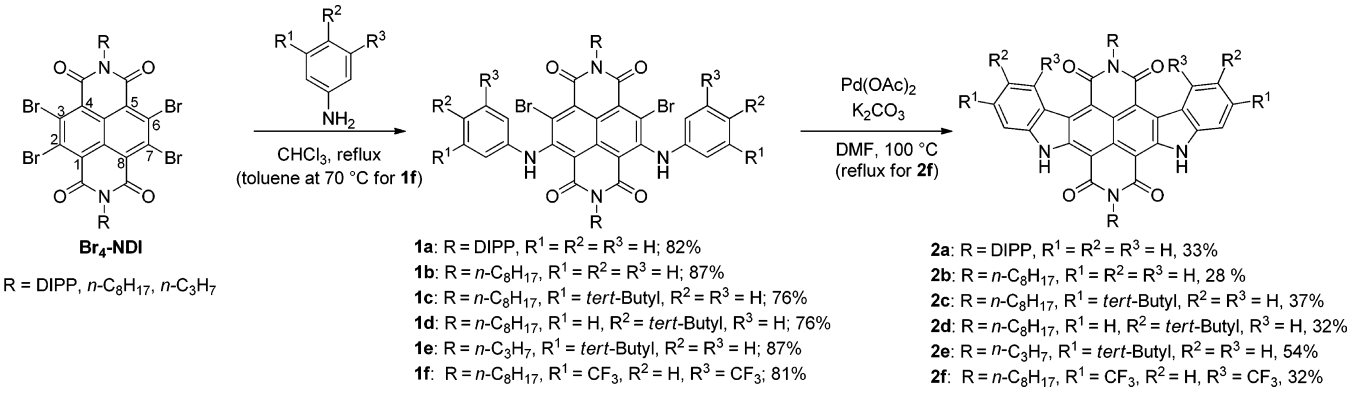

dx.doi.org/10.1021/jo402365s | J. Org. Chem. 2014, 79, 128−139

Scheme 2. Synthesis of *anti*-CbDIs 3a,b and Their Oxygen Analogues 4a and 4b and Tetraester 6

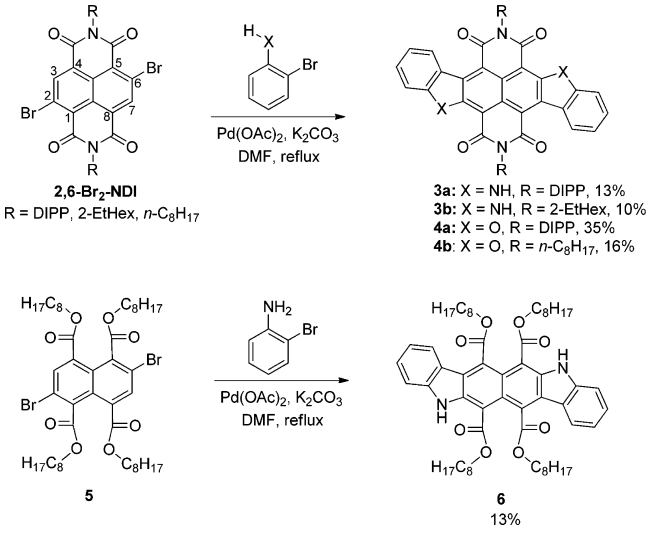

BfDI **4a** with 2,6-diisopropylphenyl groups in imide positions exhibits only poor solubility even in chlorinated solvents. The solubility of **4b** bearing an *n*-octyl group is deficient as well.

Interestingly, the present π-core expansion method is not contingent on the presence of imide groups as the reaction of 2,6-dibromonaphthalene alkylester **5**, which is accessible from isomerically pure 2,6-Br_2-NDA,[38,39] with 2-bromoaniline afforded the carbazolocarbazole **6** in 13% yield (Scheme 2).

A comparison of the ring-closure reaction of 2,7-diphenylamino-3,6-dibromo NDIs **1a–f** to *syn* and one-pot, two-step reaction of 2,6-Br_2-NDIs with 2-bromoaniline to *anti*-CbDI derivatives (Scheme 1 and 2) reveals that the former reaction can be performed under relatively milder conditions (in DMF at 100 °C) than those for the latter reaction (in refluxing DMF). Both cyclization reactions are formally of identical nature comprising a C–C coupling between a metal-activated aryl bromide and a CH-bond. However, in 2,7-diphenylamino-3,6-dibromo NDIs **1a–f** the bromine atom is located on the electron-poor aromatic unit (NDI-core) and the CH activation takes place at the electron-rich peripheral phenylamino ring. For the *anti*-isomers, presumably an intermediate is formed in situ by nucleophilic substitution of 2,6-Br_2-NDI with 2-bromoaniline that bears the bromine atoms on the phenylamino units, and hence, the situation is reversed. The differences in the required reaction conditions for *syn*- and *anti*-CbDI derivatives are in accordance with the generally accepted mechanistic assumptions[40,41] that oxidative addition of aryl bromides on palladium is facilitated by the electron-withdrawing groups, i.e., imide in the present case, and CH activation is favored for electron-rich substituents, i.e., aminophenyl. Consequently, a deactivating effect is provoked by electron-withdrawing CF_3 groups during the above-mentioned transformation of **1f** to **2f**.

We further wanted to explore the possibility of subsequent functionalization of parent CbDI, and thus investigated exemplarily the chlorination of *anti*-CbDI **3a** with *N*-chlorosuccinimide (NCS) affording a mixture of di-, tri-, and tetrachloro CbDIs (Scheme 3). ^{1}H NMR analysis revealed that the chlorination occurred exclusively at the CbDI-core and the aromatic imide substituents remained intact.

The substitution pattern of the chlorinated compounds **7a–c** could be determined by NMR analysis and is discussed later (vide infra). The TLC monitoring of the reaction indicated successive product formation; thus the substitution first takes place in the *para*-position of both carbazole amino groups, followed by chlorination in the *ortho*-position. This is in accordance with the well-established *para*- and *ortho*-directing effect of amino groups in electrophilic aromatic substitution reaction. A direct tetrachlorination of the *syn*-CbDI **2a** with NCS was also possible, exhibiting the same regioselectivity in *para*- and *ortho*-positions to the amino groups (Scheme 4).

Scheme 4. Tetrachlorination of *syn*-CbDI 2a with NCS

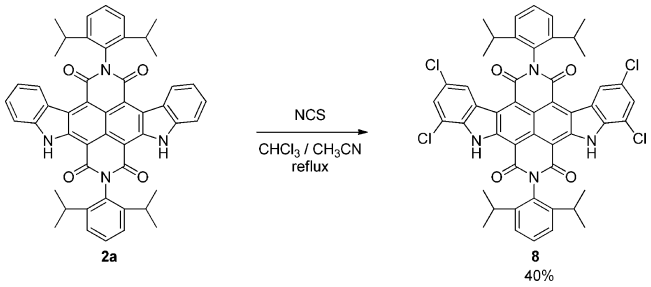

Structural Assignment by ^{1}H NMR Analysis. A common feature in the ^{1}H NMR spectra of all CbDIs (except **2f**) as well as BfDIs is a lowfield-shifted proton signal at around 9–10 ppm (for spectra, see the Supporting Information). This signal can be assigned to the H atoms in positions 1 and 8 for the *anti*-CbDIs and to the H atoms in positions 1 and 12 for the *syn*-CbDIs, respectively (Figure 1), since those protons are located in the deshielded region of the anisotropy cone of the carbonyl groups. A prerequisite for this deshielding effect is the coplanarity of the extended core and the carbonyl groups. As for the tetraester **6**, this effect is much less pronounced and the signal for the corresponding protons is found at 8.68 ppm. It is

Scheme 3. Chlorination of *anti*-CbDI 3a with NCS

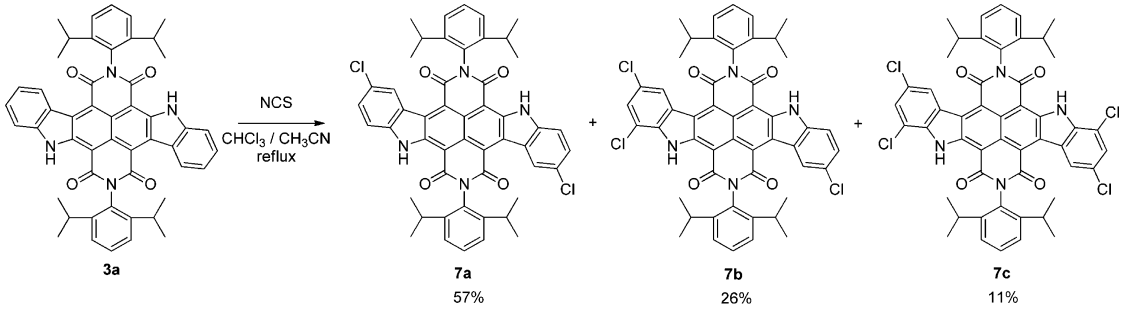

dx.doi.org/10.1021/jo402365s | J. Org. Chem. 2014, 79, 128–139

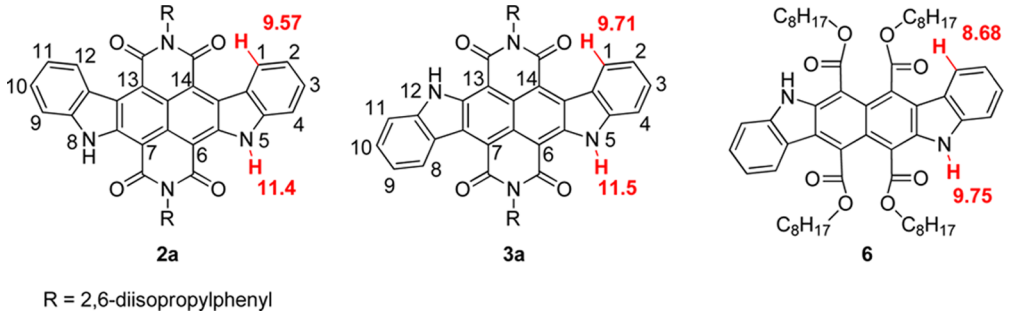

Figure 1. Structures of compounds **2a**, **3a**, and **6** with the positions and chemical shifts of the characteristic proton signals measured in CD_2Cl_2 marked.

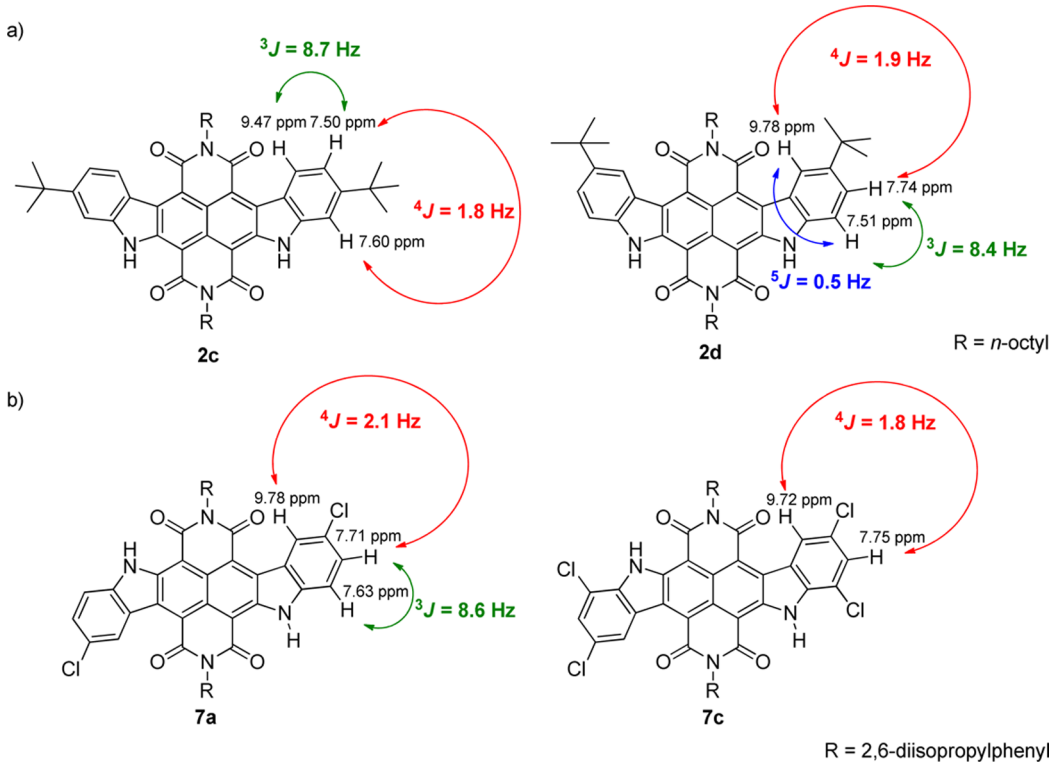

Figure 2. Structure, chemical shift, and coupling constants of relevant protons of CbDIs (a) **2c,d** and (b) **7a,c**, determined by ^{1}H NMR spectroscopy in CD_2Cl_2 and $CDCl_3$, respectively.

worthy of note that the loss of planarity in tetraester **6** also affects a highfield shift of the NH protons, compared to those of CbDIs at ca. 11.5 ppm due to the absence of the intramolecular hydrogen bonding in former compound. The lowfield shifted signal at around 9−10 ppm is helpful to determine the substitution pattern of core-substituted CbDIs in combination with the coupling pattern of the aromatic protons. For instance, the *syn*-isomers **2c** and **2d** can be distinguished by ^{1}H NMR as the protons in 1 and 12 positions show either a ^3J or a ^4J coupling, depending on the position of the *tert*-butyl group (Figure 2a). More importantly, the constitution of the chlorinated derivatives **7a**−**c** could be assigned unambiguously from the ^{1}H NMR data. While for the core-unsubstituted CbDI **3a** a doublet at 9.71 ppm with a ^3J coupling of 7.3 Hz is found, the dichlorinated compound **7a** exhibits a doublet with a smaller ^4J coupling constant of 2.1 Hz, indicating chlorination in *para*-position to the amino group (Figure 2b). The tetrachlorinated compound **7c** shows similar resonances at 9.72 and 7.75 ppm with a ^4J coupling clearly showing that the third and fourth chlorination took place at the *ortho*-position to the amino group. Based on similar considerations the structure of the tetrachloro *syn*-CbDI **8** could be assigned as well.

Structural Properties by Single-Crystal X-ray Analysis. We could unambiguously assign the *syn*- and *anti*-connectivity of indole moieties in the CbDI structure by single-crystal X-ray analyses for compounds **3a**, **2a**, **2d**, and **2e** (see Figures 3, 4, and S3−S6, Supporting Information). The single-crystal X-ray analysis of CbDI **3a** clearly reveals an *anti*-connectivity of the carbazole nitrogen atoms to the NDI-core (Figure 3a). CbDI **3a** crystallizes together with a toluene solvent molecule in a monoclinic space group $P2_1/c$ (Figures 3 and S3, Supporting Information). The enlarged NDI-core shows nearly perfect planarity with the biggest deviation observed for the carbonyl groups in the 7 and 14 positions of the CbDI core with a torsion angle of 2.9°. The proximity of the carbonyl groups to the adjacent amino group implies the formation of an intramolecular hydrogen bond, corroborated by the close N−O distance of 2.69 Å. The coplanar phenyl groups in imide

dx.doi.org/10.1021/jo402365s | J. Org. Chem. 2014, 79, 128−139

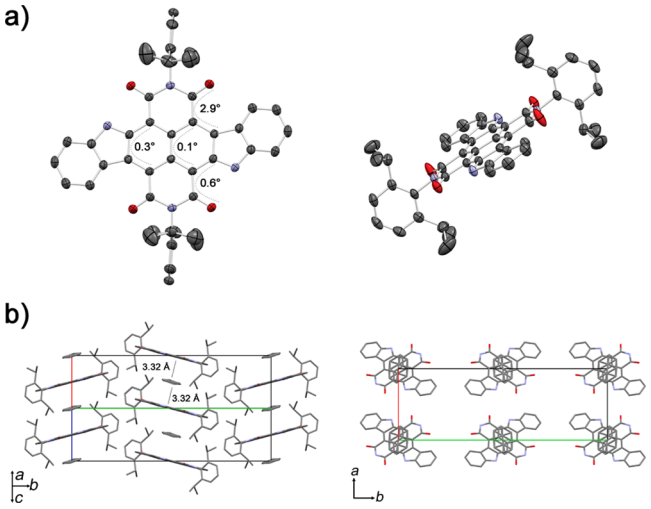

Figure 3. (a) Molecular structure with relevant torsion angles of *anti*-CbDI **3a** determined by single-crystal X-ray analysis (thermal ellipsoids are set at 50% probability) and (b) packing motif with alternating **3a** and toluene in π-stacks. Disorder of toluene is shown.

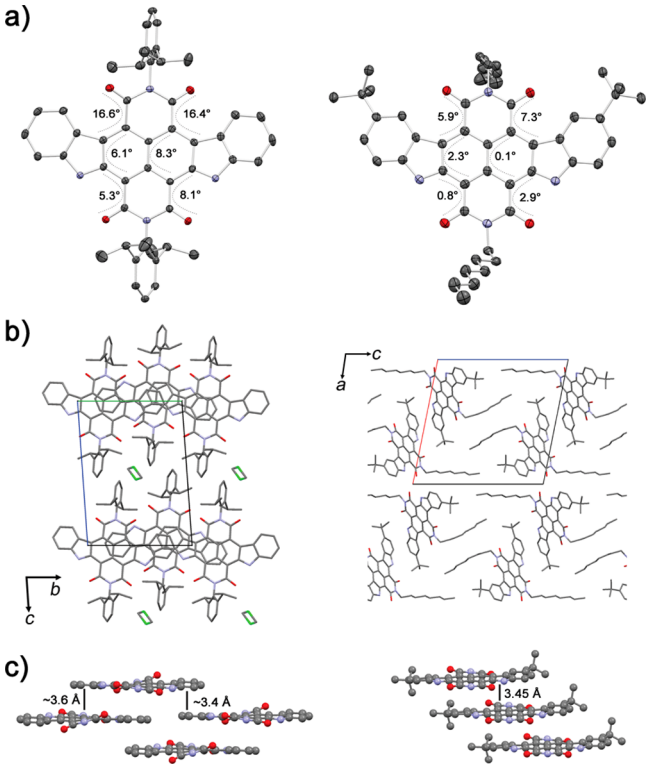

Figure 4. (a) Molecular structure with relevant torsion angles (thermal ellipsoids are set at 50% probability), (b) packing behavior, and (c) π-stacking in single crystals of CbDIs **2a** (left) and **2d** (right) determined by X-ray analysis. For CbDI **2a** dichloromethane was found as solvent inclusion.

position are oriented perpendicular to the carbazolocarbazole core. The packing motif is strongly determined by the toluene molecule. Each solvent molecule is sandwiched by two CbDIs exhibiting a close $\pi-\pi$ distance of 3.32 Å forming one-dimensional stacks separated by the imide groups (Figure 3b).

The measured single crystal of **2a** contains dichloromethane as solvent inclusion and crystallizes in the triclinic space group $P\bar{1}$ (Figures 4 and S4, Supporting Information). This crystal structure clearly shows the *syn*-connectivity of the nitrogen atoms of indole moieties. In contrast to its *anti*-isomer **3a**, the structure of the CbDI **2a** π-scaffold is not planar since the imide and naphthalene units are twisted. Conspicuously, the imide-carbonyl groups adjacent to the secondary amino groups are less twisted from planarity (torsion angles 5.3−8.1°) compared to those on the opposite side (torsion angles 16.4−16.6°). This partial planarization is apparently caused by the intramolecular hydrogen bond. Moreover, the aromatic imide substituents are not coplanar, comprising an angle of 38.6° (Figure S4, Supporting Information). The packing motif of **2a** is shown in Figure 4b,c. For this *syn*-CbDI, two-dimensional stacks of the nearly flat π-systems, resembling a brick stone arrangement, are formed, which are separated by the bulky imide substituents. The arising gaps between the 2,6-diisopropylphenyl groups are filled by the dichloromethane molecules. Within the stack a complete overlap of the enlarged NDI-core is prevented by the isopropyl groups of the bulky imide substituent, leading to four π-contacts to neighboring molecules for each CbDI. A more pronounced overlap of the π-surfaces is observed for the antiparallel neighbors, whereas the less intense $\pi-\pi$-interaction limited to the outer benzene rings is found to the parallel oriented neighboring CbDI molecules. The $\pi-\pi$ distance was determined to be 3.4−3.6 Å.

In contrast to **2a**, containing solvent inclusion of dichloromethane, for core-substituted CbDI **2d** with *n*-octyl groups in imide positions solvent-free crystals were obtained. The crystals of core-substituted CbDIs **2d** show a less distorted molecular structure than **2a** (Figures 4 and S5,6, Supporting Information). Nevertheless, also for these molecules the imide moiety adjacent to the amino groups is nearly planar, whereas the opposite side deviates from planarity with torsion angles around 6−7° for **2d**. *syn*-CbDI **2d** crystallizes in the monoclinic space group $P2_1$ (Figures 4 and S5, Supporting Information). The alkyl chain is oriented along the molecular short axis and is extended perpendicularly to the π-surface. This facilitates an intimate π-overlap between neighbors leading to a slip-stacked arrangement of parallel molecules. The stacks are extended along the *b*-axis and are assembled as pairs, enclosing an angle of 71.2°. These pairs are isolated from each other by the *n*-octyl groups (Figure S5b−d, Supporting Information) exhibiting a one-dimensional packing motif. The single crystal obtained for CbDI **2e** contains ethyl acetate as solvent inclusion, lying directly in the same plane as the CbDI molecule and forming a hydrogen bond to the amino group (Figure S6, Supporting Information). As in the case of **2d**, the CbDI **2e** forms one-dimensional stacks with intimate $\pi-\pi$-overlap due to the sterically less demanding *n*-propyl groups where antiparallel molecules are stacked on top of each other with $\pi-\pi$ distances of 3.3 and 3.5 Å, respectively.

Optical Properties. The optical properties of the new core-enlarged NDIs were investigated by UV−vis absorption spectroscopy in dichloromethane, and the results are summarized in Table 1. The UV−vis absorption spectra of *syn*-CbDI **2a**, *anti*-CbDI **3a**, and *anti*-BfDI **4a**, bearing 2,6-diisopropylphenyl groups in imide positions, are shown for comparison in Figure 5. *anti*-BfDI **4a** exhibits an absorption band in the visible region with a maximum at 474 nm and a vibronic fine structure, causing the yellow color of this chromophore in dichloromethane solution. In contrast, the CbDI derivatives absorb strongly over a broad visible region (ca. 400−660 nm). The replacement of oxygen atoms in *anti*-BfDI by secondary amino groups leads to a new bathochromic

dx.doi.org/10.1021/jo402365s | J. Org. Chem. 2014, 79, 128−139

Table 1. Optical Absorption Data and Optical Band Gaps of Core-Enlarged NDI Derivatives Measured in Dichloromethane (10^{-5} M)

	λ_{max} (nm)	ε (M^{-1} cm^{-1})	λ_{max} (nm)	ε (M^{-1} cm^{-1})	bandgap[a] (eV)
2a	531	34300	589	12400	2.10
2b	526	34600	580	11900	2.14
2c	532	40600	580[b]	11500	2.14
2d	535	31500	600[b]	9400	2.07
2e	532	40700	580[b]	11500	2.14
2f	502	26700	568	13700	2.18
3a[32]	491	38600	622	24200	1.99
3b	486	34100	615	20800	2.02
4a	474	46200	-	-	2.62
6	400	27000	500	10100	2.48
7a	483	30000	635	19900	1.95
7b	476	30400	632	19800	1.96
7c	470	30000	629	20100	1.97
8	531	28000	597	11600	2.08

[a]Calculated from the long wavelength absorption. [b]A shoulder is observed instead of a maximum.

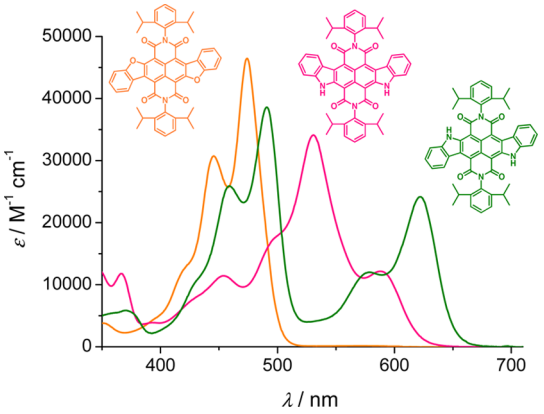

Figure 5. UV–vis absorption spectra of *anti*-BfDI **4a** (yellow), *syn*-CbDI **2a** (red), and *anti*-CbDI **3a**[32] (green) in dichloromethane (10^{-5} M).

absorption band with a maximum at 622 nm for *anti*-CbDI **3a** in addition to the blue-shifted band with a maximum at 491 nm, which is similar to the absorption band of *anti*-BfDI derivate **4a**. The occurrence of these two bands provokes, similar as for chlorophylls, the green color of **3a** solutions. Interestingly, for the corresponding *syn*-isomer CbDI **2a** the two bands apparently overlap resulting in one broad band with local maxima at 589 and 531 nm, the latter possessing the highest intensity. The solution of **2a** in dichloromethane is accordingly red in color. Noteworthy, the annulation evokes a different absorption behavior than it can be observed for core-disubstituted 2,6-diphenylamino-NDI derivatives, exhibiting a single broad absorption band at 600 nm.[35] Moreover, the emission properties of these two new derivatives **2a** and **4a** were investigated, and the fluorescence spectra are shown in Figure S1a (Supporting Information), along with that of *anti*-CbDI **3a**[32] for comparison. For *anti*-BfDI **4a**, a fluorescence quantum yield of 19% and an emission band maximum at 510 nm was observed, while the emitting CbDI **2a** (Φ_{fl} = 1%) exhibits an emission maximum at 622 nm. The emission band of the corresponding *anti*-isomer **3a** is bathochromically shifted with a maximum at 641 nm possessing a quantum yield of 5%.[32]

The UV–vis spectra of further *syn*-CbDIs **2b–e** with different substituents on the CbDI-core and *n*-octyl groups in the imide positions reveal some interesting substituent effects on the absorption properties of this new type of core-extended NDIs (Figure S1c, Supporting Information). *syn*-CbDIs **2c** and **2d** bearing *tert*-butyl groups in the *meta*- and *para*-positions to the amino groups show a slight bathochromic shift of the intensive band (from 526 to 532 and 535 nm) compared to that of respective H atom containing CbDI **2b**. The less intensive band which can be found at ca. 580 nm for both **2b** and **2c** appears as a shoulder at ca. 600 nm for derivative **2d**.

More striking is the strong blue-shift of the absorption spectrum caused by the electron-withdrawing CF_3 groups located at the *meta*-positions to the amino group of *syn*-CbDI **2f** with absorption maxima at 568 and 502 nm. Noteworthy, a similar significant blue-shift of absorption maxima was also observed for the correspondent NDI precursor **1f**, whereas *tert*-butyl groups provoke only small bathochromic shifts of absorption bands for **1c** and **1d** (Figure S1e, Supporting Information). Similarly to NDIs (Figure S1f, Supporting Information), imide substituents of CbDIs do not attain any considerable effect on their absorption properties. However, the tetraester **6** that has the same aromatic core as CbDI **3a** shows less intense but strongly blue-shifted absorption bands at 500 and 400 nm, compared to those of **3a** (see Table 1 and Figure S1d, Supporting Information).

We have also studied the optical properties of the chlorinated products **7a–c** and **8** of *anti*-CbDI **3a** and *syn*-CbDI **2a**, respectively. For the di-, tri-, and tetrachloro *anti*-CbDIs **7a–c**, a bathochromic shift up to 13 nm of the absorption band at longer wavelength was observed compared to that of the parent CbDI **3a**, whereas the absorption band at shorter wavelength is hypsochromically shifted (Figure S1b, Supporting Information, and Table 1). The tetrachlorinated *syn*-CbDI **8** exhibits only a slight red-shift of 8 nm of the less intensive band at higher wavelength in comparison to that of its parent compound **2a**. However, the highest intensity band remains unchanged at 531 nm.

Redox and Transistor Properties. Next, we investigated the redox potentials of the core-enlarged NDIs by cyclic voltammetry in dry dichloromethane with ferrocene as an internal standard (Table 2, Figures 6 and S2, Supporting Information). The results are collected in Table 2, and the CVs of *syn*-CbDI **2a**, *anti*-BfDI **4a**, and carbazolocarbazole tetraester **6** are shown in Figure 6 as representative examples for comparison (for CVs of other compounds, see Figure S2, Supporting Information). As the data in Table 2 reveal, only the reduction processes are reversible for CbDI and BfDI derivatives while the oxidation waves are either irreversible or even outside of the accessible range of our electrolyte system (>1.2 V vs Fc/Fc^+).

syn-CbDI **2a** shows indeed reduction potentials $E_{1/2}$ = −1.11 and −1.54 V very similar to those of its *anti*-isomer **3a** ($E_{1/2}$ = −1.07 and −1.49 V),[32] revealing that the structural isomers have no significant influence on the reduction behavior of these core-extended NDIs. As expected, the replacement of amino groups in CbDI **3a** by oxygen resulted in higher (less negative) reduction potentials for *anti*-BfDI **4a** with $E_{1/2}$ values of −0.94 and −1.42 V, which can be attributed to the lower donor character of oxygen compared to nitrogen. For the carbazolocarbazole derivative **6**, where the imide groups are

dx.doi.org/10.1021/jo402365s | J. Org. Chem. 2014, 79, 128–139

Table 2. Redox Properties of Core-Enlarged NDIs Determined by Cyclic Voltammetry (vs Fc/Fc^+; 100 mV s^{-1}; TBAHFP 0.1 M) and Calculated LUMO Energy

	$E_{1/2}^{Red2}$ (V)	$E_{1/2}^{Red1}$ (V)	E^{Ox1} (V)	ε(LUMO)[a] (eV)
2a	−1.54	−1.11	1.15[b]	−3.69
2b	−1.50	−1.15	1.06[b]	−3.74
2c	−1.56	−1.21	1.05[b]	−3.59
2d	−1.56	−1.19	1.02[b]	−3.61
2f	−1.27	−0.88	>1.2[c]	−3.92
3a[32]	−1.49	−1.07	1.11[b]	−3.73
4a	−1.42	−0.94	>1.2[c]	−3.86
6	−1.96	−1.74	0.73	−3.06
7a	−1.38	−0.94	>1.2[c]	−3.86
7b	−1.35	−0.90	>1.2[c]	−3.90
7c	−1.30	−0.85	>1.2[c]	−3.95
8	−1.35	−0.90	>1.2[c]	−3.90

[a]Calculated with a potential of −4.8 eV for Fc/Fc^+ against the vacuum level:[42] $\varepsilon(LUMO) = -4.8\ eV - E_{1/2}^{Red1}$. [b]Peak potential. [c]The oxidation potential could not been determined because it is beyond the accessible window of our electrolyte system.

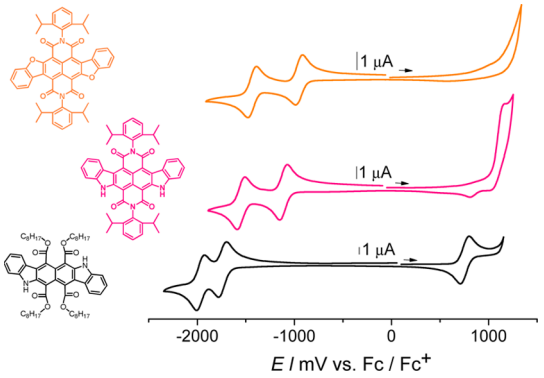

Figure 6. Cyclic voltammograms of *anti*-BfDI **4a** (yellow), *syn*-CbDI **2a** (red), and tetraester **6** (black) measured in dichloromethane by using Fc/Fc^+ couple as an internal standard (scan rate 100 mV s^{-1}; supporting electrolyte TBAHFP).

replaced by the less electron-withdrawing and less conjugated ester moieties, the redox potentials are shifted markedly to more negative values of −1.74 and −1.96 V. For this compound even a reversible oxidation was observed at 0.73 V corroborating the more electron-rich character of this π-scaffold where the four carbonyl groups are rotated out of plane.

Within the series of CbDIs bearing different substituents at the carbazole rings, electron-withdrawing groups make the corresponding derivatives more prone to reduction. Thus, the functionalization of *anti*-isomer **3a** with two, three, or four chlorine atoms to CbDI **7a**, **7b**, and **7c**, respectively, provokes a gradual increase of the reduction potentials (less negative values) from −1.07 and −1.49 V for **3a** to −0.94 and −1.38 V for **7a** to −0.85 and −1.30 V for **7c**. A similar effect was also observed for the tetrachlorinated *syn*-CbDI **8** with reduction potentials of −0.90 and −1.35 V corresponding to shifts of 0.21 and 0.19 V compared to those of parent *syn*-CbDI **2a**. A similar effect as provided by four chlorine substituents is also given by four CF_3 groups in *syn*-CbDI **2f**, which shows reduction potentials at −0.88 and −1.27 V.

The reduction potentials discussed above suggest that the LUMO level of CbDI derivatives can be tuned from ca. −3.7 eV down to nearly −4.0 eV with electron-withdrawing groups or by replacing the amino group with oxygen (Table 2). Toward a more comprehensive picture, we further calculated the frontier molecular orbitals and their energy for *syn*- and *anti*-CbDIs **2a** and **3a** as well as of the *anti*-BfDI **4a** by DFT calculations (B3-LYP). For simplicity, methyl groups instead of the 2,6-diisopropylphenyl group in the imide positions were used (for details, see Tables 3 and S1−S3, Supporting

Table 3. Calculated FMOs of *anti*-BfDI 4a, *anti*-CbDI 3a, and *syn*-CbDI 2a and the Corresponding Energy Level ε Determined by the B3-LYP-DFT Method[a]

	HOMO	LUMO	ε(HOMO) (eV) ε(LUMO) (eV)
anti-BfDI **4a**	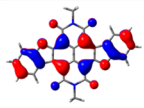	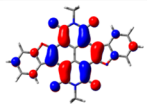	−6.55 −3.68
anti-CbDI **3a**	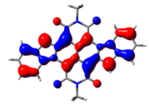	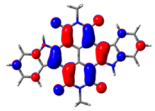	−5.91 −3.52
syn-CbDI **2a**	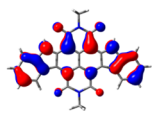	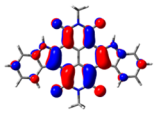	−6.02 −3.48

[a]For simplicity, methyl groups in the imide positions were used for calculations.

Information). According to these calculations, LUMO gas-phase energies are about 0.2 eV higher than those obtained from the CV data which can be explained in terms of neglected solvent effects. The trend observed for the energy levels based on CV experiments could also be found for the calculated values, showing for the *anti*-BfDI derivative a higher LUMO level of −3.68 eV than for *syn*- and *anti*-CbDI with values around −3.48 and −3.52 eV, respectively. Moreover, the *anti*-BfDI derivative has a significantly lower HOMO level of −6.55 eV compared to *syn*- and *anti*-CbDI with energies of −6.02 and −5.91 eV, respectively, as reflected by the larger optical band gap for the *anti*-BfDI derivative and the absence of an oxidation wave in our accessible electrochemical window. For all three systems, the HOMO is delocalized over the whole enlarged NDI-core, whereas the LUMO remains localized on the parent NDI unit resembling a typical LUMO of NDI derivatives.[43] We consider this last point as very important because the more widespread delocalization of the HOMO increases the chance for close contacts between HOMO orbitals of neighboring molecules in the bulk material compared to contact between LUMOs.[32] Therefore, larger transfer integrals are expected for charge transport within the HOMO manifold leading to higher p-mobility.

In our previous communication,[32] we could indeed demonstrate good hole and rather low electron mobility for *anti*-CbDI **3a** in organic thin-film transistors (TFTs) and rationalized these results on the basis of good intermolecular HOMO overlap directed by the steric demand of the bulky 2,6-diisopropylphenyl substituent in imide position, which on the other hand prohibits close spatial contacts between the LUMOs of neighboring molecules. Our preliminary results on the field effect mobilities[44] of our so far investigated new core-enlarged NDI derivatives show that the corresponding *syn*-CbDIs **2a**, along with several other derivatives, are good organic

dx.doi.org/10.1021/jo402365s | J. Org. Chem. 2014, 79, 128−139

semiconductors as well (Table S4, Supporting Information). The *syn*-isomer **2a**, whose bulky 2,6-diisopropylphenyl imide substituent direct the molecules' packing into layer structures with slipped $\pi-\pi$-contact surfaces (Figure 4c), shows a hole mobility in the same range (0.2 $cm^2/(V\ s)$) as previously reported for its *anti*-congener.[32] Like for **3a**, we could also observe n-channel transport for OTFTs of **2a** with one to 2 orders of magnitude lower mobility that complies with our expectations based on the slipped packing arrangement in the crystals, which owing to the transversal offset of the NDI cores cannot provide significant LUMO−LUMO overlap (Figure 4c).

Whereas for CbDIs **2a** and **3a**[32] ambipolar transport properties with superior p-channel transport was observed, *anti*-BfDI **4a** with the same imide substituent (DIPP) shows only n-type behavior with appreciable mobility up to 0.06 $cm^2/(V\ s)$. This observation is in good accordance with the lowered FMO levels (Tables 2 and S1, Supporting Information) of the oxygen analogue, where n-type behavior is now provided by the low LUMO level close to −3.9 eV while the too deep lying HOMO level disfavors charge injection for p-transport from the gold electrode. A similar trend is also found for *syn*-CbDIs **2b** and **2f** with *n*-octyl groups in imide position. The former derivative, and similarly the *tert*-butyl substituted derivatives **2c** and **2d**, exhibits only p-type behavior with hole mobility of 10^{-2} $cm^2/(V\ s)$, whereas for CF_3-substituted derivative **2f** with its low LUMO level of −3.92 eV only n-type behavior with electron mobility of up to 10^{-3} $cm^2/(V\ s)$ was measured. With regard to our transistor measurements, we have to point out, however, that we could not achieve the high quality thin films for several of our new molecules so far, which obviously makes a comparison of the given mobility values in terms of HOMO−HOMO or LUMO−LUMO contacts impossible. Unfortunately, we are as yet not in the position to carry out the measurements under inert atmosphere but only under ambient conditions, where only for very densely packed molecules in closed multilayers can n-channel transport be achieved for molecules with a LUMO level above a value of around −3.9 eV[45] (earlier work even considered −4.3 eV as the upper limit).[18] Obviously **2a** and **3a** with rather high LUMO levels of −3.7 eV have to exhibit such densely packed layers that enable ambient n-channel operation despite the absence of commonly applied fluoroalkyl chains to repel the penetration of humidity. Accordingly, more in-depth studies on the utilization of CbDI and BfDI compounds in transistor devices are strongly motivated and will be addressed in our future research.

CONCLUSION

We have synthesized a series of core-enlarged NDI derivatives consisting of six annulated rings bearing heteroatoms. In particular, a selective synthetic route to unknown *syn*-CbDIs is presented, completing the series of core-extended NDIs with annulated indole moieties. For further tuning the electronic properties, we have synthesized core-functionalized CbDIs, either starting from precursors containing the desired functional groups or by subsequent functionalization of the parent CbDI, particularly by chlorination. Furthermore, oxygen analogues to the *anti*-CbDIs with benzofurofuran units were synthesized. Single-crystal X-ray analyses confirmed unambiguously the *syn*- and *anti*-connectivity in CbDI derivatives and revealed the influence of imide substituents on the π-stacking of these compounds in the solid state. The optical and electrochemical properties of CbDI derivatives are shown to be dependent on their structural features. The hereby synthesized core-extended NDI derivatives are highly promising organic semiconductors whose HOMO and LUMO levels can be tuned toward p- or n-channel transport.

EXPERIMENTAL SECTION

Materials and Methods. 2,6-Dibromonaphthalenetetracarboxylic dianhydride (2,6-Br_2-NDA),[35] *N,N′*-bis(2,6-diisopropylphenyl)-2,6-dibromonaphthalenetetracarboxylic acid diimide (2,6-Br_2-NDI-DIPP),[46] *N,N′*-bis(2-ethylhexyl)-2,6-dibromonaphthalenetetracarboxylic acid diimide (2,6-Br_2-NDI-Ethex),[47] *N,N′*-di-(*n*-octyl)-2,3,6,7-tetrabromonaphthalenetetracarboxylic acid diimide (Br_4-NDI-C_8H_{17}),[48] and *N,N′*-bis(2′,6′-diisopropylphenyl)-2,3,6,7-tetrabromonaphthalenetetracarboxylic acid diimide (Br_4-NDI-DIPP)[49] were synthesized according to the literature procedures. Aniline was distilled under argon and stored under exclusion of light. DMF was dried over P_2O_5 and stored under argon and exclusion of light. All other reagents and solvents were obtained from commercial suppliers and purified and dried according to standard procedures.[50] Column chromatography was performed on silica gel (particle size 0.040−0.063 mm). A preparative recycling GPC with 2H + 2.5H columns was used for further purification. Solvents for spectroscopic studies were of spectroscopic grade and used as received. For cyclic voltammetry measurements, a standard commercial electrochemical analyzer with a three-electrode single-compartment cell was used. Dichloromethane (HPLC grade) was dried over calcium hydride under argon and degassed before use. The supporting electrolyte tetrabutylammonium hexafluorophosphate (TBAHFP) was prepared according to the literature[51] and recrystallized from ethanol/water. The measurements were carried out in dichloromethane at a concentration of $<10^{-4}$ M with ferrocene (Fc) as an internal standard for the calibration of the potential. A Ag/AgCl reference electrode was used. A Pt disc and a Pt wire were applied as working and auxiliary electrodes, respectively. UV−vis measurements were performed in a conventional quartz cell (light pass 10 mm) on a standard, commercial spectrometer. Fluorescence quantum yields were determined under dilute conditions in CH_2Cl_2 ($<10^{-6}$ M) versus *N,N′*-bis(2,6-diisopropylphenyl)-1,6,7,12-tetraphenoxyperylene-3,4:9,10-tetracarboxylic acid bisimide (Φ_{fl} = 0.96 in $CHCl_3$)[52] or *N,N′*-bis(2,6-diisopropylphenyl)-3,4:9,10-tetracarboxylic acid bisimide (Φ_{fl} = 1 in $CHCl_3$).[53] ^1H and ^{13}C spectra were recorded in CD_2Cl_2 or $CDCl_3$ on a 400 or 600 MHz spectrometer. Residual undeuterated solvent was used as internal standard. High-resolution mass spectra were measured by ESI-TOF and EI experiments. The measurements of single crystals of **2a**, **2d**, and **2e** were performed on a diffractometer with a CMOS APS detector under monochromated Cu Kα radiation. The crystal data of **3a** were collected on a diffractometer with a CCD area detector and graphite-monochromated Mo Kα radiation. The structures were solved using direct methods, refined with the SHELX software package[54] and expanded using Fourier techniques. All non-hydrogen atoms were refined anisotropically. Hydrogen atoms were included in structure factors calculations. All hydrogen atoms were assigned to idealized geometric positions.

*N,N′-Bis(2′,6′-diisopropylphenyl)-2,7-dibromo-3,6-diphenylamino-1,4,5,8-naphthalenetetracarboxylic Acid Diimide (**1a**).* To a solution of Br_4-NDI-DIPP (149 mg, 0.165 mg) in chloroform (50 mL) was added aniline (1.8 mL). The solution was refluxed for 40 min, the solvent was removed under reduced pressure, and the residue was purified by column chromatography (dichloromethane/pentane 1:1) yielding a dark blue solid (162 mg, 82%). Mp: 285−288 °C. ^1H NMR (400 MHz, CD_2Cl_2): 11.84 (s, 2H, NH) 7.53−7.47 (m, 2H), 7.37−7.31 (m, 8H), 7.16 (t, ^3J = 7.6 Hz, 2H), 7.07 (d, ^3J = 7.6 Hz, 4H), 2.77 (sept, ^3J = 6.8 Hz, 2H), 2.65 (sept, ^3J = 6.8 Hz, 2H), 1.18 (d, ^3J = 6.8 Hz, 12H), 1.11 (d, ^3J = 6.8 Hz, 12H). ^{13}C NMR (101 MHz, CD_2Cl_2): 165.3, 161.7, 151.6, 146.3, 146.1, 141.9, 131.3, 131.0, 130.2, 129.5, 128.5, 125.1, 124.64, 124.56, 122.1, 119.8, 119.0, 108.3, 29.8, 29.6, 24.1, 24.0. HRMS (ESI, acetonitrile/chloroform, pos mode): *m/z* 925.1960 $[M + H]^+$, calcd for $C_{50}H_{47}Br_2N_4O_4$ 925.1959. UV−vis (CH_2Cl_2): λ_{max}/nm ($\varepsilon/M^{-1}\ cm^{-1}$) = 570 (23500).

dx.doi.org/10.1021/jo402365s | J. Org. Chem. 2014, 79, 128−139

*N,N′-Di(n-octyl)-2,7-dibromo-3,6-diphenylamino-1,4,5,8-naphthalenetetracarboxylic Acid Diimide (**1b**).* To a solution of Br_4-NDI-C_8H_{17} (170 mg, 0.211 mmol) in chloroform (50 mL) was added aniline (1.8 mL) was added. The solution was refluxed for 2 h, the solvent was removed under reduced pressure, and the residue was purified by column chromatography (dichloromethane/pentane 1:1) yielding a dark blue solid (153 mg, 87%). The product obtained by an alternative procedure was previously described and characterized.[37]

*N,N′-Di(n-octyl)-2,7-dibromo-3,6-di(3-tert-butylphenylamino)-naphthalenetetracarboxylic Acid Diimide (**1c**).* To a solution of Br_4-NDI-C_8H_{17} (144 mg, 0.179 mmol) in chloroform (10 mL) was added 3-*tert*-butylaniline (0.2 mL, 1.26 mmol). The solution was refluxed for 45 min, the solvent was removed under reduced pressure, and the residue was purified by column chromatography (dichloromethane/pentane 1:1) yielding a dark blue solid (129 mg, 76%). Mp: 135−137 °C. ^{1}H NMR (400 MHz, $CDCl_3$): 12.09 (s, 2H, NH), 7.25 (dd, ^3J = 7.8 Hz, 2H), 7.18 (ddd, ^3J = 7.8 Hz, ^4J = 1.6 Hz, ^4J = 1.0 Hz, 2H), 7.07 (dd, ^4J = 1.8 Hz, 2H), 6.82 (ddd, ^3J = 7.8 Hz, ^4J = 2.2 Hz, ^4J = 1.0 Hz, 2H), 4.20 (t, ^3J = 7.7 Hz, 2H), 4.15 (t, ^3J = 7.7 Hz, 2H), 1.79−1.67 (m, 4H), 1.47−1.17 (m, 38H), 0.90−0.82 (m, 6H). ^{13}C NMR (101 MHz, $CDCl_3$): 164.7, 161.1, 152.5, 151.06, 141.2, 128.81, 128.79, 127.2, 121.8, 118.8, 118.7, 118.6, 118.5, 107.7, 42.4, 41.4, 34.9, 31.9, 31.4, 29.8, 29.44, 29.39, 29.34, 28.1, 27.9, 27.4, 27.3, 22.77, 22.75, 14.23, 14.21. HRMS (ESI, acetonitrile/chloroform, pos mode): m/z 941.3216 $[M + H]^+$ calcd for $C_{50}H_{63}Br_2N_4O_4$ 941.3211. UV−vis (CH_2Cl_2): λ_{max}/nm (ε/M^{-1} cm^{-1}) = 573 (22100).

*N,N′-Di-(n-octyl)-2,7-dibromo-3,6-di(4-tert-butylphenylamino)-1,4,5,8-naphthalenetetracarboxylic Acid Diimide (**1d**).* To a solution of Br_4−NDI-C_8H_{17} (199 mg, 0.247 mg) in chloroform (30 mL) 4-*tert*-butylaniline (0.1 mL, 0.63 mmol) was added. The solution was refluxed for 3 h 15 min, the solvent was removed under reduced pressure and the residue was purified by column chromatography (dichloromethane/pentane 1:1) yielding a dark blue solid (177 mg, 76%); mp 205−206 °C. ^{1}H NMR (400 MHz, $CDCl_3$): 12.0 (bs, 2H), 7.37−7.30 (m, 4H), 6.99−6.93 (m, 4H), 4.24−4.08 (m, 4H), 1.82−1.62 (m, 4H), 1.45−1.17 (m, 38H), 0.92−0.82 (m, 6H). ^{13}C NMR (101 MHz, $CDCl_3$): 164.6, 161.1, 151.3, 147.9, 139.1, 128.8, 126.9, 126.2, 121.3, 118.9, 118.5, 107.7, 42.5, 42.3, 34.6, 31.9, 31.5, 29.4, 29.3, 28.1, 27.9, 27.4, 27.3, 22.8, 22.7, 14.22, 14.21. HRMS (ESI, acetonitrile/chloroform, pos mode): m/z 941.3209 $[M + H]^+$, calcd for $C_{50}H_{63}Br_2N_4O_4$: 941.3211. UV−vis (CH_2Cl_2): λ_{max}/nm (ε/M^{-1} cm^{-1}) = 575 (22600).

N,N′-Di(n-propyl)-2,3,6,7-tetrabromo-1,4,5,8-naphthalenetetracarboxylic Acid Diimide. Br_4-NDA (3.0 g, 5.1 mmol) and *n*-propylamine (1.3 mL, 16 mmol) were refluxed in acetic acid (40 mL) for 40 min. After addition of a second portion on amine (0.6 mL, 7 mmol), the mixture was refluxed for further 20 min and poured into water (150 mL). The resulting precipitate was filtered off and dried. Then it was suspended in dry toluene (200 mL), and PBr_3 (3 mL) was added. The mixture was refluxed for 8 h, and the solvent was removed under reduced pressure. The residue was dissolved in dichloromethane (60 mL) and washed with water (2 × 50 mL), and the organic phases were combined. After evaporation of solvent, the crude product was purified by column chromatography (dichloromethane/pentane 1:1) yielding a yellow crystalline solid (89 mg, 3%). Mp: 338−340 °C. ^{1}H NMR (400 MHz, CD_2Cl_2): 4.24−4.12 (m, 4H), 1.86−1.76 (m, 4H), 1.04 (t, ^3J = 7.4 Hz, 6H). ^{13}C NMR (101 MHz, $CDCl_3$): 160.0, 135.8, 126.8, 125.8, 44.5, 21.5, 11.6. HRMS (ESI, acetonitrile/chloroform, pos mode): m/z 662.7757 $[M + H]^+$, calcd for $C_{20}H_{15}Br_4N_2O_4$ 662.7760. UV−vis (CH_2Cl_2): λ_{max}/nm (ε/M^{-1} cm^{-1}) = 425 (13800).

*N,N′-Di(n-propyl)-2,7-dibromo-3,6-di(3-tert-butylphenylamino)-1,4,5,8-naphthalenetetracarboxylic Acid Diimide (**1e**).* To a solution of Br_4-NDI-C_3H_7 (81.1 mg, 0.122 mmol) in chloroform (10 mL) was added 3-*tert*-butylaniline (0.14 mL, 0.88 mmol). The solution was refluxed for 2 h, the solvent was removed under reduced pressure, and the residue was purified by column chromatography (dichloromethane/pentane 4:1) yielding a dark blue solid (85 mg, 87%). Mp: 263 °C. ^{1}H NMR (400 MHz, $CDCl_3$): 12.1 (s, 2H), 7.25 (t, ^3J = 7.8 Hz, 2H), 7.18 (d, ^3J = 7.8 Hz, 2H), 7.07 (t, ^4J = 2.0 Hz, 2H), 6.83 (d, ^3J = 8.0 Hz, 2H), 4.24−4.16 (m,2H), 4.16−4.08 (m, 2H) (m, 4H), 1.85−1.70 (m, 4H), 1.31 (s, 9H), 1.02 (t, ^3J = 7.4 Hz, 3H), 1.01 (t, ^3J = 7.4 Hz, 3H). ^{13}C NMR (101 MHz, $CDCl_3$): 164.8, 161.1, 152.5, 151.1, 141.2, 128.8, 127.2, 121.8, 118.81, 118.76, 118.6, 107.7, 43.8, 42.8, 34.9, 31.4, 21.4, 21.2, 11.7, 11.6. HRMS (ESI, acetonitrile/chloroform, pos mode): m/z 801.1650 $[M + H]^+$, calcd for $C_{40}H_{43}Br_2N_4O_4$ 801.1646. UV−vis (CH_2Cl_2): λ_{max}/nm (ε/M^{-1} cm^{-1}) = 573 (23100).

*N,N′-Di(n-octyl)-2,7-bis((3,5-bis(trifluormethyl)phenyl)amino)-3,6-dibromo-1,4,5,8-naphthalenetetracarboxylic Acid Diimide (**1f**).* To a solution of Br_4-NDI-C_8H_{17} (72.3 mg, 89.8 μmol) in toluene (5 mL) was added 3,5-bis(trifluoromethyl)aniline (0.2 mL, 1.2 mmol). The solution was stirred at 70 °C for 4 d, and a second portion of the amine (0.1 mL, 0.6 mmol) was added. After a further 2 d, the solvent was removed under reduced pressure and the residue was purified by column chromatography (dichloromethane/pentane 1:4) yielding a red solid (80.6 mg, 81%). Mp: 192−196 °C. ^{1}H NMR (400 MHz, $CDCl_3$): 12.00 (s, 2H), 7.63 (s, 2H), 7.38 (s, 4H), 4.26−4.17 (m, 4H), 1.82−1.68 (m, 4H), 1.47−1.19 (m, 20H), 0.92−0.81 (m, 6H). ^{13}C NMR (101 MHz, $CDCl_3$): 164.6, 160.4, 149.6, 143.1, 132.8 (^2J(C,F) = 34 Hz), 128.1, 127.4, 123.2 (^1J(C,F) = 275 Hz), 120.65, 120.62, 120.59, 117.6, 110.0, 42.8, 41.9, 31.91, 31.89, 29.9, 29.4, 29.34, 29.30, 28.1, 27.8, 27.32, 27.29, 22.8, 22.7, 14.21, 14.17. HRMS (ESI, acetonitrile/chloroform, pos mode): m/z 1101.1457 $[M + H]^+$, calcd for $C_{46}H_{43}Br_2F_{12}N_4O_4$ 1101.1454. UV−vis (CH_2Cl_2): λ_{max}/nm (ε/M^{-1} cm^{-1}) = 535 (23900).

*N,N′-Bis(2,6-diisopropylphenyl)-5H,8H-carbazolo[2,3-b]-carbazole[6,7:13,14]tetracarboxylic Acid Diimide (**2a**).* NDI **1a** (76.2 mg, 82.2 μmol), K_2CO_3 (22.8 mg, 0.165 mmol), and $Pd(OAc)_2$ (5.4 mg, 26 μmol) were placed under argon, and dry DMF (5 mL) was added. The reaction mixture was stirred for 60 min at 100 °C. After removal of the solvent under reduced pressure, the residue was purified by column chromatography (dichloromethane/pentane 1:1) yielding a dark red solid (20.8 mg, 33%). Mp: >400 °C. ^{1}H NMR (400 MHz, CD_2Cl_2): δ = 11.4 (s, 2H), 9.57 (dd, ^3J = 8.16 Hz, ^4J = 0.76 Hz, 2H), 7.73−7.66 (m, 4H), 7.66−7.57 (m, 2H), 7.49 (d, ^3J = 7.6 Hz, 2H), 7.46 (d, ^3J = 7.6 Hz, 2H), 7.41−7.37 (m, 2H), 2.98 (sept, ^3J = 6.8 Hz, 2H), 2.87 (sept, ^3J = 6.8 Hz, 2H), 1.22 (d, ^3J = 6.8 Hz, 12H), 1.20 (d, ^3J = 6.8 Hz, 12H).^{13}C NMR (100 MHz, CD_2Cl_2): 166.0, 164.9, 146.71, 146.66, 144.5, 144.1, 132.0, 131.0, 130.9, 130.20, 130.15, 130.0, 128.8, 125.8, 124.8, 124.6, 122.5, 122.1, 121.6, 118.8, 111.8, 103.3, 29.8, 29.7, 24.2, 24.1. HRMS (ESI, acetonitrile/chloroform, pos mode): m/z 765.3437 $[M + H]^+$, calcd for $C_{50}H_{45}N_4O_4$ 765.3435. UV−vis (CH_2Cl_2): λ_{max}/nm (ε/M^{-1} cm^{-1}) = 589 (12400), 531 (34300). Fluorescence (CH_2Cl_2, λ_{ex} = 516 nm): λ_{max} = 622 nm; Φ_{fl} = 1%. CV (CH_2Cl_2, 0.1 M TBAHFP, vs Fc/Fc^+): $E_{1/2}^{Red2}$ = −1.54 V, $E_{1/2}^{Red1}$ = −1.11 V, E_p^{Ox}(X/X^+) = 1.15 V.

*N,N′-Di(n-octyl)-5H,8H-carbazolo[2,3-b]carbazole[6,7:13,14]-tetracarboxylic Acid Diimide (**2b**).* NDI **1b** (153 mg, 0.184 mmol), K_2CO_3 (102 mg, 0.738 mmol), and $Pd(OAc)_2$ (14 mg, 62 μmol) were placed under argon, and dry DMF (10 mL) was added. The reaction mixture was stirred for 80 min at 100 °C. After removal of the solvent under reduced pressure, the residue was purified by column chromatography (chloroform/hexane 1:1) yielding a dark red solid (35 mg, 28%). Mp: 273−274 °C. ^{1}H NMR (400 MHz, $CDCl_3$): 11.1 (s, 2H, NH), 9.51 (d, ^3J = 8.4 Hz, 2H), 7.55 (t, ^3J = 7.8 Hz, 2H), 7.43−7.32 (m, 4H), 4.35−4.20 (m, 4H), 1.92−1.78 (m, 4H), 1.52−1.19 (m, 20H), 0.89 (t, ^3J = 6.9 Hz, 6H). ^{13}C NMR (151 MHz, $CDCl_3$): 163.3, 163.8, 143.5, 143.3, 130.4, 129.8, 127.6, 124.0, 121.84, 121.77, 121.3, 117.2, 111.2, 102.2, 41.6, 40.4, 32.03, 32.00, 29.59, 29.58, 29.48, 29.45, 28.40, 28.35, 27.54, 27.50, 22.83, 22.81, 14.3. HRMS (APCI, acetonitrile/chloroform 1:1, pos mode): m/z 669.3434 $[M + H]^+$, calcd for $C_{42}H_{45}N_4O_4$ 669.3435. UV−vis (CH_2Cl_2): λ_{max}/nm (ε/M^{-1} cm^{-1}) = 580 (11900), 526 (34600). CV (CH_2Cl_2, 0.1 M TBAHFP, vs Fc/Fc^+): $E_{1/2}^{Red2}$ = −1.50 V, $E_{1/2}^{Red1}$ = −1.15 V, E_p^{Ox}(X/X^+) = 1.06 V.

*N,N′-Di(n-octyl)-5H,8H-3,10-di-tert-butylcarbazolo[2,3-b]-carbazole[6,7:13,14]tetracarboxylic Acid Diimide (**2c**).* NDI **1c** (99.0 mg, 0.105 mmol), K_2CO_3 (29.0 mg, 0.210 mmol), and $Pd(OAc)_2$ (7.0 mg, 31 μmol) were placed under argon, and dry DMF (7 mL) was added. The reaction mixture was stirred for 60 min at 100 °C. After

dx.doi.org/10.1021/jo402365s | J. Org. Chem. 2014, 79, 128−139

removal of the solvent under reduced pressure, the residue was purified by column chromatography (dichloromethane/pentane 1:1) yielding a dark red solid (30 mg, 37%). Mp: 353−355 °C. ^{1}H NMR (400 MHz, CD_2Cl_2): 11.16 (s, 2H, NH), 9.47 (d, ^3J = 8.7 Hz, 2H), 7.60 (d, ^4J = 1.8 Hz, 2H), 7.50 (dd, ^3J = 8.7 Hz, ^4J = 1.8 Hz, 2H), 4.13−4.02 (m, 4H), 1.82−1.68 (m, 4H), 1.52 (s, 9H), 1.50−1.24 (m, 18H), 0.93−0.84 (m, 6H). ^{13}C NMR (151 MHz, $CDCl_3$): 165.1, 163.7, 154.7, 144.0, 143.7, 129.5, 127.5, 123.5, 121.1, 119.8, 119.0, 117.1, 108.0, 102.0, 41.2, 40.1, 35.6, 32.02, 31.99, 31.6, 29.6, 29.54, 29.45, 29.42, 28.34, 28.3, 27.5, 27.4, 22.83, 22.81, 14.26. HRMS (ESI, acetonitrile/chloroform, pos mode): m/z 780.4607 $[M]^+$, calcd for $C_{50}H_{60}N_4O_4$: 780.4609. UV−vis (CH_2Cl_2): λ_{max}/nm (ε/M^{-1} cm^{-1}) = 532 (40600). CV (CH_2Cl_2, 0.1 M TBAHFP, vs Fc/Fc^+): $E_{1/2}^{Red2}$ = −1.56 V, $E_{1/2}^{Red1}$ = −1.21 V, $E_p^{Ox}(X/X^+)$ = 1.05 V.

*N,N′-Di(n-octyl)-5H,8H-2,11-di-tert-butylcarbazolo[2,3-b]-carbazole[6,7:13,14]tetracarboxylic Acid Diimide (**2d**).* NDI **1d** (160 mg, 0.170 mmol), K_2CO_3 (48.0 mg, 0.347 mmol), and $PdOAc_2$ (11.1 mg, 49.4 μmol) were placed under argon, and dry DMF (8 mL) was added. The reaction mixture was stirred for 60 min at 100 °C. After removal of the solvent under reduced pressure, the residue was purified by column chromatography (dichloromethane/pentane 1:1) yielding a dark red solid (42.8 mg, 32%). Mp: 285−288 °C. ^{1}H NMR (400 MHz, CD_2Cl_2): 11.25 (s, 2H), 9.78 (d, ^4J = 2.0 Hz, 2H), 7.74 (dd, ^3J = 8.4 Hz, ^4J = 2.0 Hz, 2H), 7.51 (dd, ^3J = 8.4 Hz, ^5J = 0.5 Hz, 2H), 4.43 (t, ^3J = 7.5 Hz, 2H), 4.30 (t, ^3J = 7.5 Hz, 2H), 2.00−1.88 (m, 2H), 1.88−1.76 (m, 2H), 1.55 (s, 9H), 1.52−1.22 (m, 20H), 0.92−0.85 (m, 6H). ^{13}C NMR (101 MHz, $CDCl_3$): 165.5, 164.0, 144.5, 144.0, 141.4, 128.2, 127.9, 126.2, 122.1, 121.3, 117.1, 110.6, 102.0, 41.3, 40.3, 35.4, 32.2, 32.1, 32.0, 29.6, 29.45, 29.44, 29.36, 28.4, 28.2, 27.6, 27.3, 22.83, 22.80, 14.27, 14.25. HRMS (ESI, acetonitrile/chloroform, pos mode): m/z 780.4607 $[M]^+$, calcd for $C_{50}H_{60}N_4O_4$: 780.4609. UV−vis (CH_2Cl_2): λ_{max}/nm (ε/M^{-1} cm^{-1}) = 535 (31500). CV (CH_2Cl_2, 0.1 M TBAHFP, vs Fc/Fc^+): $E_{1/2}^{Red2}$ = −1.56 V, $E_{1/2}^{Red1}$ = −1.19 V, $E_p^{Ox}(X/X^+)$ = 1.02 V.

*N,N′-Di(n-propyl)-5H,8H-3,10-di-tert-butylcarbazolo[2,3-b]-carbazole[6,7:13,14]tetracarboxylic Acid Diimide (**2e**).* NDI **1e** (76.0 mg, 95.0 μmol), K_2CO_3 (26.5 mg, 0.192 mmol), and $Pd(OAc)_2$ (6.0 mg, 27 μmol) were placed under argon and dry DMF (7 mL) was added. The reaction mixture was stirred for 90 min at 100 °C. After removal of the solvent under reduced pressure, the residue was purified by column chromatography (dichloromethane/pentane 1:1) yielding a dark red solid (33.0 mg, 54%). Mp: 399−402 °C. ^{1}H NMR (400 MHz, CD_2Cl_2): 11.11 (s, 2H), 9.44 (d, ^3J = 8.7 Hz, 2H), 7.59 (d, ^4J = 1.8 Hz, 2H), 7.50 (dd, ^3J = 8.7 Hz, ^4J = 1.8 Hz, 2H), 4.05−3.98 (m, 4H), 1.82−1.69 (m, 4H), 1.52 (s, 18H), 1.08−0.98 (m, 6H). ^{13}C NMR (101 MHz, $CDCl_3$): 165.2, 163.8, 154.8, 144.0, 143.7, 129.5, 127.6, 123.5, 121.1, 119.8, 119.0, 117.1, 107.9, 102.0, 42.7, 41.5, 35.6, 31.6, 21.6, 21.5, 11.83, 11.78. HRMS (APCI, dichloromethane, pos mode): m/z 640.3058 $[M]^+$, calcd for $C_{40}H_{40}N_4O_4$: 640.3044. UV−vis (CH_2Cl_2): λ_{max}/nm (ε/M^{-1} cm^{-1}) = 532 (40700).

*N,N′-Di(n-octyl)-5H,8H-1,3,10,12-tetrakis(trifluoromethyl)-carbazolo[2,3-b]carbazole[6,7:13,14]tetracarboxylic Acid Diimide (**2f**).* NDI **1f** (83.8 mg, 76.0 μmol), K_2CO_3 (21.5 mg, 0.156 mmol), and $Pd(OAc)_2$ (5.2 mg, 23 μmol) were placed under argon, and dry DMF (5 mL) was added. The reaction mixture was stirred for 45 min at 100 °C. Since no product formation was detected by TLC, the mixture was refluxed for 1 h. After removal of the solvent under reduced pressure, the residue was purified by column chromatography (dichloromethane/pentane 1:1) yielding a dark red solid (22.8 mg, 32%). Mp: 216−220 °C. ^{1}H NMR (400 MHz, $CDCl_3$): 11.3 (s, 2H), 8.03 (s, 2H), 7.92 (s, 2H), 4.36−4.25 (m, 2H), 4.21 (t, ^3J = 7.4 Hz,2H), 2.01 (tt, ^3J = 6.8 Hz, 2H), 1.77 (tt, ^3J = 6.8 Hz, 2H), 1.62−1.18 (m, 20H), 0.93 −0.83 (m, 6H). ^{13}C NMR (151 MHz, $CDCl_3$): 164.5, 164.2, 144.7, 143.3, 131.7 (^2J(C,F) = 34 Hz), 129.8 (^2J(C,F) = 34 Hz), 127.7, 125.9, 123.9 (^1J(C,F) = 272 Hz), 123.4 (^1J(C,F) = 272 Hz), 123.1, 120.5, 118.7, 111.9 (^3J(C,F) = 3.9 Hz), 42.7, 40.4, 31.98, 31.95, 29.5, 29.37, 29.35, 29.3, 28.3, 28.1, 27.3, 27.2, 22.82, 22.78, 14.24, 14.23. HRMS (ESI, acetonitrile/chloroform, pos mode): m/z 941.2929 $[M + H]^+$, calcd for $C_{46}H_{41}F_{12}N_4O_4$ 941.2931. UV−vis (CH_2Cl_2): λ_{max}/nm (ε/M^{-1} cm^{-1}) = 568 (13700), 502 (26700). CV (CH_2Cl_2, 0.1 M TBAHFP, vs Fc/Fc^+): $E_{1/2}^{Red2}$ = −1.27 V, $E_{1/2}^{Red1}$ = −0.88 V.

*N,N′-Bis(2,6-diisopropylphenyl)-5H,12H-carbazolo[2,3-b]-carbazole[6,7:13,14]tetracarboxylic Acid Diimide (**3a**).* 2,6-Br_2-NDI-DIPP (60.0 mg, 80.6 μmol), 2-bromoaniline (38.8 mg, 0.226 mmol), $Pd(OAc)_2$ (4.0 mg, 17.8 μmol), PCy_3 (11.0 mg, 35.4 μmol), and Cs_2CO_3 (52.2 mg, 16.2 μmol) were placed in dry dimethylacetamide (5 mL) under argon atmosphere and stirred for 1 h at 125 °C and an additional 1 h at 175 °C. The solvent was removed under reduced pressure, and the residual crude product was purified by column chromatography (dichloromethane/pentane 1:1) and recycling GPC yielding a dark green solid (3.0 mg, 8%), mp >400 °C. The product obtained by an alternative procedure was previously described and characterized.[32]

*N,N′-Bis(2-ethylhexyl)-5H,12H-carbazolo[2,3-b]carbazole-[6,7:13,14]tetracarboxylic Acid Diimide (**3b**).* 2,6-Br_2-NDI-EtHex (156 mg, 0.241 mmol), 2-bromoaniline (177 mg, 0.680 mmol), $Pd(OAc)_2$ (18.2 mg, 81.1 μmol), and K_2CO_3 (66.0 mg, 0.478 mmol) were placed under argon, and dry DMF (10 mL) was added. The mixture was refluxed for 50 min, and DMF was removed under reduced pressure. The residue was purified by column chromatography (dichloromethane/pentane 1:1) yielding a dark green solid (16 mg, 10%). Mp: 359−360 °C. ^{1}H NMR (400 MHz, $CDCl_3$): 11.52 (s, 2H), 9.76 (d, ^3J = 8.1 Hz, 2H), 7.70−7.68 (m, 2H), 7.56 (d, ^3J = 8.0 Hz, 2H), 7.46−7.41 (m, 2H), 4.42−4.21 (m, 4H), 2.19−2.01 (m, 2H), 1.50−1.27 (m, 16H), 0.99 (t, ^3J = 7.2 Hz, 6H), 0.90 (t, ^3J = 7.4 Hz, 6H). ^{13}C NMR (151 MHz, $CDCl_3$): 165.8, 164.3, 144.2, 142.0, 131.0, 130.3, 130.1, 121.4, 121.0, 120.7, 119.4, 111.2, 104.4, 44.5, 38.1, 31.0, 28.8, 24.3, 23.3, 14.3, 10.9. HRMS (ESI, acetonitrile/chloroform, pos mode): m/z 669.3437 $[M + H]^+$, calcd for $C_{42}H_{45}N_4O_4$ 669.3435. UV−vis (CH_2Cl_2): λ_{max}/nm (ε/M^{-1} cm^{-1}) = 615 (20800), 486 (34100).

*N,N′-Bis(2,6-diisopropylphenyl)benzofuro[2,3-b]benzofuran-[6,7:13,14]tetracarboxylic Acid Diimide (**4a**).* 2,6-Br_2-NDI-DIPP (200 mg, 0.268 mmol), 2-bromophenol (0.08 mL, 0.75 mmol), $Pd(OAc)_2$ (18.0 mg, 80.6 μmol), and K_2CO_3 (74.0 mg, 0.537 mmol) were placed under argon in dry DMF (15 mL) and refluxed for 3 h. The solvent was removed under reduced pressure, and the residue was purified by column chromatography (dichloromethane/pentane 2:1) and washing with hot chloroform yielding a yellow solid (73.0 mg, 35%). Mp: >400 °C. ^{1}H NMR (400 MHz, CD_2Cl_2): 9.53 (ddd, ^3J = 8.3 Hz, ^4J = 1.4 Hz, ^5J = 0.6 Hz, 2H), 7.81 (ddd, ^3J = 8.5 Hz, ^4J = 1.2 Hz, ^5J = 0.6 Hz, 2H), 7.84−7.79 (m, 2H), 7.61 (t, ^3J = 7.7 Hz, 2H), 7.56−7.50 (m, 2H), 7.46 (d, ^3J = 7.7 Hz, 4H), 2.89 (sept, ^3J = 6.8 Hz, 4H), 1.22 (d, ^3J = 6.84 Hz, 12H), 1.19 (d, ^3J = 6.84 Hz, 12H). ^{13}C (151 MHz, $CDCl_3$, 55 °C): 163.8, 161.0, 160.7, 157.7, 146.1, 132.9, 132.8, 130.8, 130.5, 130.1, 124.6, 134.5, 134.3, 121.4, 120.8, 112.4, 109.1, 29.73, 24.24, 24.18. HRMS (ESI, acetonitrile/chloroform, pos mode): m/z 767.3119 $[M + H]^+$, calcd for $C_{50}H_{43}N_2O_6$ 767.3116. UV−vis (CH_2Cl_2): λ_{max}/nm (ε/M^{-1} cm^{-1}) = 474 (46200). Fluorescence (CH_2Cl_2, λ_{ex} = 445 nm): λ_{max} = 502 nm; Φ_{fl} = 19%. CV (CH_2Cl_2, 0.1 M TBAHFP, vs Fc/Fc^+): $E_{1/2}^{Red2}$ = −1.42 V, $E_{1/2}^{Red1}$ = −0.94 V.

*N,N′-Di(n-octyl)benzofuro[2,3-b]benzofuran[6,7:13,14]-tetracarboxylic Acid Diimide (**4b**).* 2,6-Br_2-NDI-C_8H_{17} (180 mg, 0.278 mmol), 2-bromophenol (0.08 mL, 0.750 mmol) $Pd(OAc)_2$ (18.7 mg, 83.3 μmol), and K_2CO_3 (76.6 mg, 0.554 mmol) were placed under argon in dry DMF (7 mL) and refluxed for 3 h. The solvent was removed under reduced pressure, and the residue was purified by column chromatography (dichloromethane) yielding a yellow solid (30.1 mg, 16%). Mp: 376−378 °C. ^{1}H NMR (600 MHz, $C_2D_2Cl_4$, 78 °C): 9.61 (d, ^3J = 7.8 Hz, 2H), 7.85 (d, ^3J = 7.8 Hz, 2H), 7.78−7.73 (m, 2H), 7.58−7.51 (m, 2H), 4.36 (t, ^3J = 7.8 Hz, 4H), 1.88 (tt, ^3J = 7.8 Hz, 4H), 1.55−1.20 (m, 10H), 0.86 (t, ^3J = 7.1 Hz, 6H).^{13}C NMR (151 MHz, $C_2D_2Cl_4$, 78 °C): 163.4, 161.1, 160.5, 157.2, 132.8, 132.3, 130.3, 124.6, 123.4, 121.3, 120.7, 112.3, 108.9, 41.4, 32.0, 29.6, 29.4, 28.4, 27.6, 22.8, 14.25. HRMS (EI, 70 eV): m/z 670.3030, calcd for $C_{42}H_{42}N_2O_6$: 670.3037. UV−vis (CH_2Cl_2): λ_{max}/nm (ε/M^{-1} cm^{-1}) = 470 (54000).

dx.doi.org/10.1021/jo402365s | J. Org. Chem. 2014, 79, 128−139

*2,6-Dibromonaphthalene-1,4,5,8-tetracarboxylic Acid n-Octyl Ester (**5**).* 2,6-Br_2-NDA (2.13 g, 5.00 mmol) was added to a solution of KOH (1.4 g, 25 mmol) in water (400 mL) and stirred for 30 min at room temperature. 1-Bromooctane (8.0 mL, 46 mmol) and tetra(*n*-octyl)ammonium bromide (2.0 g, 3.7 mmol) were added, and the mixture was refluxed for 2.5 h. After the mixture was cooled to room temperature, the aqueous mixture was extracted with dichloromethane and the aqueous phase was washed with dichloromethane. The organic phases were combined, the solvent was removed under reduced pressure, and the residue was purified by column chromatography (dichloromethane/pentane 1:3) yielding a colorless oil (1.62 g, 36%). ^{1}H NMR (400 MHz, $CDCl_3$): 8.05 (s, 2H), 4.30 (t, ^3J = 6.8 Hz, 8H), 1.82−1.73 (m, 8H), 1.49−1.22 (m, 40H), 0.90−0.85 (m, 12H). ^{13}C NMR (101 MHz, $CDCl_3$): 166.6, 166.5, 134.61, 134.57, 132.9, 128.7, 121.3, 66.7, 66.6, 31.9, 29.36, 29.34, 29.31, 29,30, 28.6, 28.4, 26.2, 26.0, 22.9, 14.2. HRMS (ESI, acetonitrile/chloroform, pos mode): *m*/*z* 947.3074 $[M + K]^+$, calcd for $C_{46}H_{70}Br_2KO_8$ 947.3069.

*Tetraoctyl 5,12-Dihydrocarbazolo[3,2-b]carbazole-6,7,13,14-tetracarboxylate (**6**).* Tetetraester **5** (142 mg, 0.156 mmol), 2-bromoaniline (76.0 mg, 0.442 mmol), $Pd(OAc)_2$ (10.5 mg, 46.8 μmol), and K_2CO_3 (43.8 mg, 0.317 mmol) were placed under argon. After addition of dry DMF (10 mL), the mixture was refluxed for 40 min. The solvent was removed under reduced pressure, and the residue was purified by column chromatography (dichloromethane/pentane 1:1) and HPLC (NP, chloroform) yielding an orange solid (19 mg, 13%). Mp: 70−77 °C. ^{1}H NMR (400 MHz, CD_2Cl_2): 9.75 (s, 2H), 8.68 (d, ^3J = 8.2 Hz, 2H), 7.61−7.56 (m, 2H), 7.51 (d, ^3J = 8.1 Hz, 2H), 7.32−7.23 (m, 2H), 4.50−4.35 (m, 8H), 1.84−1.62 (m, 8H), 1.42−1.12 (m, 40H), 0.85−0.74 (m, 12H). ^{13}C NMR (101 MHz, $CDCl_3$): 168.5, 168.0, 143.5, 140.2, 129.5, 126.3, 126.2, 123.5, 121.2, 120.4, 110.6, 109.7, 65.7, 65.6, 31.9, 29.33, 29.32, 29.2, 28.67, 28.66, 26.05, 26.04, 22.72, 22.71, 14.16. HRMS (ESI, acetonitrile/chloroform, pos mode): *m*/*z* 930.5755 $[M]^+$, calcd for $C_{58}H_{78}N_2O_8$: 930.5753. UV−vis (CH_2Cl_2): λ_{max}/nm (ε/M^{-1} cm^{-1}) = 500 (10100), 400 (27000). CV (CH_2Cl_2, 0.1 M TBAHFP, vs Fc/Fc^+): $E_{1/2}^{Red2}$ = −1.96 V, $E_{1/2}^{Red1}$ = −1.74 V, $E_{1/2}^{Ox}$ = 0.73 V.

Chlorination of CbDI Derivative 3a. CbDI **3a** (24.0 mg, 36.6 μmol) and *N*-chlorosuccinimide (20.0 mg, 0.150 mol) were dissolved in a mixture of chloroform (10 mL) and acetonitrile (10 mL) and refluxed for 5 d. After removal of the solvent under reduced pressure, the residue was purified by column chromatography (dichloromethane/pentane 1:1) yielding the following compounds.

*N,N′-Bis(2,6-diisopropylphenyl)-5H,12H-2,9-dichlorocarbazolo-[2,3-b]carbazole[6,7:13,14]tetracarboxylic Acid Diimide (**7a**).* Green solid: 15 mg (57%). Mp: >400 °C. ^{1}H NMR (400 MHz, $CDCl_3$): 11.55 (s, 2H), 9.78 (d, ^4J = 1.8 Hz, 2H), 7.68 (dd, ^3J = 8.5 Hz, ^4J = 2.0 Hz), 7.64 (t, ^3J = 7.6 Hz, 2H), 7.52 (d, ^3J = 8.4 Hz, ^5J = 0.5 Hz, 2H), 7.49 (d, ^3J = 7.8 Hz, 4H), 2.87 (sept, ^3J = 6.9 Hz, 4H), 1.26−1.21 (m, 24H). ^{13}C NMR (101 MHz, $CDCl_3$): 165.7, 164.1, 145.9, 142.9, 142.8, 131.7, 130.5, 130.31, 130.29, 129.9, 127.3, 124.6, 122.2, 122.1, 120.3, 112.2, 105.0, 29.61, 24.22, 24.14. HRMS (ESI, acetonitrile/chloroform, pos mode): *m*/*z* 833.2660 $[M + H]^+$, calcd for $C_{50}H_{43}Cl_2N_4O_4$ 833.2656. UV−vis (CH_2Cl_2): λ_{max}/nm (ε/M^{-1} cm^{-1}) = 635 (19900), 483 (30000). CV (CH_2Cl_2, 0.1 M TBAHFP, vs Fc/Fc^+): $E_{1/2}^{Red2}$ = −1.38 V, $E_{1/2}^{Red1}$ = −0.94 V.

*N,N′-Bis(2,6-diisopropylphenyl)-5H,12H-2,4,9-trichlorocarbazolo-[2,3-b]carbazole[6,7:13,14]tetracarboxylic Acid Diimide (**7b**).* Green solid: 7.0 mg (26%). Mp: >400 °C.^{1}H NMR (400 MHz, CD_2Cl_2): 11.64 (s, 1H), 11.58 (s, 1H), 9.74 (d, ^4J = 2.0 Hz, 1H), 9.68 (dd, ^4J = 2.0 Hz, ^5J = 0.68 Hz, 1H), 7.76 (d, ^4J = 2.0 Hz, 1H), 7.72 (dd, ^3J = 8.6 Hz, ^4J = 2.0 Hz, 2H), 7.66−7.60 (m, 3H), 7.48 (d, ^3J = 7.8 Hz, 2H), 7.48 (d, ^3J = 7.8 Hz, 2H), 2.95−2.83 (m, 4H), 1.26−1.19 (m, 24H). ^{13}C NMR (151 MHz, $CDCl_3$): 165.6, 165.5, 164.0, 145.92, 145.89, 143.2, 142.9, 142.1, 140.2, 132.0. 130.9, 130.5, 130.42, 130.40, 130.37, 130.34, 130.06, 130.05, 128.5, 127.5, 127.1, 124.8, 124.7, 123.1, 122.48, 122.46, 122.1, 120.8, 120.4, 117.0, 112.3, 105.9, 104.9, 29.66, 29.63, 24.3, 24.24, 24.16, 24.1. HRMS (ESI, acetonitrile/chloroform, neg mode): *m*/*z* 865.2125 $[M - H]^-$, calcd for $C_{50}H_{40}Cl_3N_4O_4$: 868.2121. UV−vis (CH_2Cl_2): λ_{max}/nm (ε/M^{-1} cm^{-1}) = 632 (19800), 476 (30400). CV (CH_2Cl_2, 0.1 M TBAHFP, vs Fc/Fc^+): $E_{1/2}^{Red2}$ = −1.35 V, $E_{1/2}^{Red1}$ = −0.90 V.

*N,N′-Bis(2,6-diisopropylphenyl)-5H,12H-2,4,9,11-tetrachlorocarbazolo[2,3-b]carbazole[6,7:13,14]tetracarboxylic Acid Diimide (**7c**).* Green solid: 3 mg (11%). Mp: >400 °C. ^{1}H NMR (400 MHz, $CDCl_3$): 11.7 (s, 2H), 9.72 (d, ^4J = 1.8 Hz, ^5J = 0.6 Hz, 2H), 7.75 (d, ^4J = 1.8 Hz, 2H), 7.65 (t, ^3J = 7.8 Hz, 2H), 7.50 (d, ^3J = 7.8 Hz, 4H), 2.86 (sept, ^3J = 6.8 Hz, 4H), 1.24 (2xd, ^3J = 6.9 Hz, 24H). ^{13}C NMR (151 MHz, $CDCl_3$): 165.4, 163.9, 145.9, 142.4, 140.3, 130.7, 130.63, 130.56, 130.2, 128.6, 127.3, 124.8, 123.0, 122.7, 120.9, 117.1, 105.7, 29.7, 24.3, 24.1. HRMS (APCI, dichloromethane, pos mode): *m*/*z* 901.1869 $[M + H]^+$, calcd for $C_{50}H_{41}Cl_4N_4O_4$ 901.1876. UV−vis (CH_2Cl_2): λ_{max}/nm (ε/M^{-1} cm^{-1}) = 629 (20100), 470 (30000). CV (CH_2Cl_2, 0.1 M TBAHFP, vs Fc/Fc^+): $E_{1/2}^{Red2}$ = −1.30 V, $E_{1/2}^{Red1}$ = −0.85 V.

*N,N′-Bis(2,6-diisopropylphenyl)-5H,8H-2,4,7,9-tetrachlorocarbazolo[2,3-b]carbazole[6,7:13,14]tetracarboxylic Acid Diimide (**8**).* CbDI **2a** (53.5 mg, 69.9 μmol) and *N*-chlorosuccinimide (40.0 mg, 0.300 mmol) were dissolved in a mixture of chloroform (8 mL) and acetonitrile (10 mL) and refluxed for 3 d. After addition of a further portion of *N*-chlorosuccinimide (120 mg, 0.900 mmol), the reaction was refluxed again for 8 h. The solvent was removed under reduced pressure, and the residue was purified by column chromatography and HPLC (dichloromethane/pentane 1:1). The tetrachloro product was obtained as a dark red solid (25 mg, 40%). Mp: >400 °C. ^{1}H NMR (400 MHz, CD_2Cl_2): 11.55 (s, 2H), 9.55 (dd, ^4J = 1.8 Hz, ^5J = 0.5 Hz, 2H), 7.75 (d, ^4J = 1.8 Hz, 2H), 7.65 (t, ^3J = 7.5 Hz, 1H), 7.61 (t, ^3J = 7.5 Hz, 1H), 7.55−7.42 (m, 4H), 2.91 (sept, ^3J = 6.8 Hz, 2H), 2.84 (sept, ^3J = 6.8 Hz, 2H), 1.22 (t, ^3J = 6.8 Hz, 2H), 1.21 (t, ^3J = 6.8 Hz, 2H). ^{13}C NMR (151 MHz, $CDCl_3$): 165.3, 163.9, 145.9, 145.8, 144.1, 139.6, 130.8, 130.6, 130.5, 130.1, 129.6, 128.2, 128.0, 127.7, 126.2, 124.8, 124.7, 123.6, 123.5, 119.2, 117.2, 103.7, 29.8, 29.6, 24.22, 24.19. HRMS (ESI, acetonitrile/chloroform, pos mode): *m*/*z* 901.1881 $[M + H]^+$, calcd for $C_{50}H_{41}Cl_4N_4O_4$ 901.1877. UV−vis (CH_2Cl_2): λ_{max}/nm (ε/M^{-1} cm^{-1}) = 597 (11600), 531 (28000). CV (CH_2Cl_2, 0.1 M TBAHFP, vs Fc/Fc^+): $E_{1/2}^{Red2}$ = −1.35 V, $E_{1/2}^{Red1}$ = −0.90 V.

■ ASSOCIATED CONTENT

Ⓢ Supporting Information

Figures S1−S6 and Tables S1−S4 mentioned in the text, NMR spectra of new compounds (Figures S7−S48), and CIF files of compounds **3a** (CCDC 965679), **2a** (CCDC 965680), **2d** (CCDC 965681), and **2e** (CCDC 965682). This material is available free of charge via the Internet at http://pubs.acs.org.

■ AUTHOR INFORMATION

Corresponding Author

*Fax: +49 (0)931 31 84756. Tel: +49 (0)931 31 85340. E-mail: wuerthner@chemie.uni-wuerzburg.de.

Notes

The authors declare no competing financial interest.

■ ACKNOWLEDGMENTS

We thank Hagen Klauk and Ute Zschieschang for the evaluation of the transistor properties. Financial support by the German Ministry of Education and Research (BMBF) for this work within the project POLYTOS (FKZ: 13N10205) in the Leading Edge Cluster “Forum Organic Electronics” is gratefully acknowledged.

■ REFERENCES

(1) Facchetti, A. *Mater. Today* **2007**, *10*, 28−37.
(2) Mas-Torrent, M.; Rovira, C. *Chem. Soc. Rev.* **2008**, *37*, 827−838.
(3) Wu, W.; Liu, Y.; Zhu, D. *Chem. Soc. Rev.* **2010**, *39*, 1489−1502.

(4) Wang, C.; Dong, H.; Hu, W.; Liu, Y.; Zhu, D. *Chem. Rev.* **2012**, *112*, 2208−2267.
(5) Mei, J.; Diao, Y.; Appleton, A. L.; Fang, L.; Bao, Z. *J. Am. Chem. Soc.* **2013**, *135*, 6724−6746.
(6) Coropceanu, V.; Cornil, J.; da Silva Filho, D. A.; Olivier, Y.; Silbey, R.; Brédas, J.-L. *Chem. Rev.* **2007**, *107*, 926−952.
(7) Anthony, J. E. *Angew. Chem., Int. Ed.* **2008**, *47*, 452−483.
(8) Anthony, J. E. *Chem. Rev.* **2006**, *106*, 5028−5048.
(9) Takimiya, K.; Ebata, H.; Sakamoto, K.; Izawa, T.; Otsubo, T.; Kunugi, Y. *J. Am. Chem. Soc.* **2006**, *128*, 12604−12605.
(10) Tang, M. L.; Reichardt, A. D.; Siegrist, T.; Mannsfeld, S. C. B.; Bao, Z. *Chem. Mater.* **2008**, *20*, 4669−4676.
(11) Subramanian, S.; Park, S. K.; Parkin, S. R.; Podzorov, V.; Jackson, T. N.; Anthony, J. E. *J. Am. Chem. Soc.* **2008**, *130*, 2706−2707.
(12) Gao, P.; Beckmann, D.; Tsao, H. N.; Feng, X.; Enkelmann, V.; Baumgarten, M.; Pisula, W.; Müllen, K. *Adv. Mater.* **2009**, *21*, 213−216.
(13) Niimi, K.; Shinamura, S.; Osaka, I.; Miyazaki, E.; Takimiya, K. *J. Am. Chem. Soc.* **2011**, *133*, 8732−8739.
(14) Jiang, W.; Li, Y.; Wang, Z. *Chem. Soc. Rev.* **2013**, *42*, 6113−6127.
(15) Anthony, J. E.; Brooks, J. S.; Eaton, D. L.; Parkin, S. R. *J. Am. Chem. Soc.* **2001**, *123*, 9482−9483.
(16) Park, S. K.; Jackson, T. N.; Anthony, J. E.; Mourey, D. A. *Appl. Phys. Lett.* **2007**, *91*, 063514.
(17) Sakanoue, T.; Sirringhaus, H. *Nat. Mater.* **2010**, *9*, 736−740.
(18) Jones, B. A.; Facchetti, A.; Wasielewski, M. R.; Marks, T. J. *J. Am. Chem. Soc.* **2007**, *129*, 15259−15278.
(19) Würthner, F.; Stolte, M. *Chem. Commun.* **2011**, *47*, 5109−5115.
(20) Zhan, X.; Facchetti, A.; Barlow, S.; Marks, T. J.; Ratner, M. A.; Wasielewski, M. R.; Marder, S. R. *Adv. Mater.* **2011**, *23*, 268−284.
(21) Katsuta, S.; Tanaka, K.; Maruya, Y.; Mori, S.; Masuo, S.; Okujima, T.; Uno, H.; Nakayama, K.; Yamada, H. *Chem. Commun.* **2011**, *47*, 10112−10114.
(22) Yue, W.; Gao, J.; Li, Y.; Jiang, W.; Di Motta, S.; Negri, F.; Wang, Z. *J. Am. Chem. Soc.* **2011**, *133*, 18054−18057.
(23) Mohebbi, A. R.; Munoz, C.; Wudl, F. *Org. Lett.* **2011**, *13*, 2560−2563.
(24) Doria, F.; di Antonio, M.; Benotti, M.; Verga, D.; Freccero, M. *J. Org. Chem.* **2009**, *74*, 8616−8625.
(25) Langhals, H.; Kinzel, S. *J. Org. Chem.* **2010**, *75*, 7781−7784.
(26) Hu, Y.; Gao, X.; Di, C.; Yang, X.; Zhang, F.; Liu, Y.; Li, H.; Zhu, D. *Chem. Mater.* **2011**, *23*, 1204−1215.
(27) Cai, K.; Yan, Q.; Zhao, D. *Chem. Sci.* **2012**, *3*, 3175−3182.
(28) Chen, X.; Guo, Y.; Tan, L.; Yang, G.; Li, Y.; Zhang, G.; Liu, Z.; Xu, W.; Zhang, D. *J. Mater. Chem. C* **2013**, *1*, 1087−1092.
(29) Gao, X.; Di, C.; Hu, Y.; Yang, X.; Fan, H.; Zhang, F.; Liu, Y.; Li, H.; Zhu, D. *J. Am. Chem. Soc.* **2010**, *132*, 3697−3699.
(30) Zhao, Y.; Di, C.; Gao, X.; Hu, Y.; Guo, Y.; Zhang, L.; Liu, Y.; Wang, J.; Hu, W.; Zhu, D. *Adv. Mater.* **2011**, *23*, 2448−2453.
(31) Zhang, F.; Hu, Y.; Schuettfort, T.; Di, C.; Gao, X.; McNeill, C. R.; Thomsen, L.; Mannsfeld, S. C. B.; Yuan, W.; Sirringhaus, H.; Zhu, D. *J. Am. Chem. Soc.* **2013**, *135*, 2338−2349.
(32) Suraru, S.-L.; Zschieschang, U.; Klauk, H.; Würthner, F. *Chem. Commun.* **2011**, *47*, 11504−11506.
(33) Gao, J.; Li, Y.; Wang, Z. *Org. Lett.* **2013**, *15*, 1366−1369.
(34) Fukutomi, Y.; Nakano, M.; Hu, J.-Y.; Osaka, I.; Takimiya, K. *J. Am. Chem. Soc.* **2013**, *135*, 11445−11448.
(35) Thalacker, C.; Röger, C.; Würthner, F. *J. Org. Chem.* **2006**, *71*, 8098−8105.
(36) Vollmann, H.; Becker, H.; Corell, M.; Streeck, H. *Liebigs Ann.* **1937**, *531*, 1−159.
(37) Suraru, S.-L.; Würthner, F. *J. Org. Chem.* **2013**, *78*, 5227−5238.
(38) Kishore, R. S. K.; Ravikumar, V.; Bernardinelli, G.; Sakai, N.; Matile, S. *J. Org. Chem.* **2007**, *73*, 738−740.
(39) Yuan, Z.; Li, J.; Xiao, Y.; Li, Z.; Qian, X. *J. Org. Chem.* **2010**, *75*, 3007−3016.
(40) Alberico, D.; Scott, M. E.; Lautens, M. *Chem. Rev.* **2007**, *107*, 174−238.
(41) Ackermann, L.; Vicente, R.; Kapdi, A. R. *Angew. Chem., Int. Ed.* **2009**, *48*, 9792−9826.
(42) D'Andrade, B. W.; Datta, S.; Forrest, S. R.; Djurovich, P.; Polikarpov, E.; Thompson, M. E. *Org. Electron.* **2005**, *6*, 11−20.
(43) Würthner, F.; Ahmed, S.; Thalacker, C.; Debaerdemaeker, T. *Chem.—Eur. J.* **2002**, *8*, 4742−4750.
(44) The experimental setup for OTFT preparation and characterization was identical to the one described previously; see ref 32.
(45) Schmidt, R.; Oh, J. H.; Sun, Y.-S.; Deppisch, M.; Krause, A.-M.; Radacki, K.; Braunschweig, H.; Könemann, M.; Erk, P.; Bao, Z.; Wurthner, F. *J. Am. Chem. Soc.* **2009**, *131*, 6215−6228.
(46) Chopin, S.; Chaignon, F.; Blart, E.; Odobel, F. *J. Mater. Chem.* **2007**, *17*, 4139−4146.
(47) Guo, X.; Watson, M. D. *Org. Lett.* **2008**, *10*, 5333−5336.
(48) Gao, X.; Qiu, W.; Yang, X.; Liu, Y.; Wang, Y.; Zhang, H.; Qi, T.; Liu, Y.; Lu, K.; Du, C.; Shuai, Z.; Yu, G.; Zhu, D. *Org. Lett.* **2007**, *9*, 3917−3920.
(49) Röger, C.; Würthner, F. *J. Org. Chem.* **2007**, *72*, 8070−8075.
(50) Perrin, D. D.; Armarego, W. L.; Perrin, D. R. *Purification of Laboratory Chemicals*, 2nd ed.; Pergamon Press, Ltd.: Oxford, 1980.
(51) Fry, A. J. In *Laboratory Techniques in Electroanalytical Chemistry*, 2nd ed.; Kissinger, P., Heineman, W. R., Eds.; Marcel Dekker Ltd.: New York, 1996.
(52) Gvishi, R.; Reisfeld, R.; Burshtein, Z. *Chem. Phys. Lett.* **1993**, 213.
(53) Seybold, G.; Wagenblast, G. *Dyes Pigm.* **1989**, *11*, 303−317.
(54) Sheldrick, G. *Acta Crystallogr., Sect. A* **2008**, *64*, 112−122.